Neuropsychopharmacology (2016) 41, 1034–1045

www.neuropsychopharmacology.org

CFH Variants Affect Structural and Functional Brain Changes and Genetic Risk of Alzheimer's Disease

Deng-Feng Zhang[1,2], Jin Li[3], Huan Wu[2,4], Yue Cui[3], Rui Bi[1], He-Jiang Zhou[1], Hui-Zhen Wang[1], Chen Zhang[5], Dong Wang[1], Alzheimer's Disease Neuroimaging Initiative (ADNI)[10], Qing-Peng Kong[4], Tao Li[6], Yiru Fang[5], Tianzi Jiang*[,3,7,8,9] and Yong-Gang Yao*[,1,2,7]

[1]Key Laboratory of Animal Models and Human Disease Mechanisms of the Chinese Academy of Sciences and Yunnan Province, Kunming Institute of Zoology, Chinese Academy of Sciences, Kunming, China; [2]Kunming College of Life Science, University of Chinese Academy of Sciences, Kunming, China; [3]Brainnetome Center and National Laboratory of Pattern Recognition, Institute of Automation, Chinese Academy of Sciences, Beijing, China; [4]State Key Laboratory of Genetic Resources and Evolution, Kunming Institute of Zoology, Chinese Academy of Sciences, Kunming , China; [5]Division of Mood Disorders, Shanghai Mental Health Center, Shanghai Jiao Tong University School of Medicine, Shanghai, China; [6]Mental Health Center and Psychiatric Laboratory, West China Hospital, Sichuan University, Chengdu, China; [7]CAS Center for Excellence in Brain Science and Intelligence Technology, Chinese Academy of Sciences, Shanghai, China; [8]Key Laboratory for NeuroInformation of Ministry of Education, School of Life Science and Technology, University of Electronic Science and Technology of China, Chengdu, China; [9]Queensland Brain Institute, University of Queensland, Brisbane, Australia

The immune response is highly active in Alzheimer's disease (AD). Identification of genetic risk contributed by immune genes to AD may provide essential insight for the prognosis, diagnosis, and treatment of this neurodegenerative disease. In this study, we performed a genetic screening for AD-related top immune genes identified in Europeans in a Chinese cohort, followed by a multiple-stage study focusing on *Complement Factor H* (*CFH*) gene. Effects of the risk SNPs on AD-related neuroimaging endophenotypes were evaluated through magnetic resonance imaging scan, and the effects on AD cerebrospinal fluid biomarkers (CSF) and *CFH* expression changes were measured in aged and AD brain tissues and AD cellular models. Our results showed that the AD-associated top immune genes reported in Europeans (*CR1*, *CD33*, *CLU,* and *TREML2*) have weak effects in Chinese, whereas *CFH* showed strong effects. In particular, rs1061170 ($P_{meta} = 5.0 \times 10^{-4}$) and rs800292 ($P_{meta} = 1.3 \times 10^{-5}$) showed robust associations with AD, which were confirmed in multiple world-wide sample sets (4317 cases and 16 795 controls). Rs1061170 ($P = 2.5 \times 10^{-3}$) and rs800292 ($P = 4.7 \times 10^{-4}$) risk-allele carriers have an increased entorhinal thickness in their young age and a higher atrophy rate as the disease progresses. Rs800292 risk-allele carriers have higher CSF tau and Aβ levels and severe cognitive decline. *CFH* expression level, which was affected by the risk-alleles, was increased in AD brains and cellular models. These comprehensive analyses suggested that CFH is an important immune factor in AD and affects multiple pathological changes in early life and during disease progress.

Neuropsychopharmacology (2016) **41,** 1034–1045; doi:10.1038/npp.2015.232; published online 26 August 2015

*Correspondence: Dr T Jiang, Brainnetome Center and National Laboratory of Pattern Recognition, Institute of Automation, Chinese Academy of Sciences, Beijing 100190, China, Tel: +86 10 8254 4778, Fax: +86 10 8254 4777, E-mail: jiangtz@nlpr.ia.ac.cn or Dr Y-G Yao, Key Laboratory of Animal Models and Human Disease Mechanisms of the Chinese Academy of Sciences and Yunnan Province, Kunming Institute of Zoology, Chinese Academy of Sciences, Kunming 650204, China, Tel: +86 871 65180085, Fax: +86 871 65180085,
E-mail: yaoyg@mail.kiz.ac.cn

[10]Data used in preparation of this article were partly obtained from the Alzheimer's Disease Neuroimaging Initiative (ADNI) database (adni.loni.usc.edu). As such, the investigators within the ADNI contributed to the design and implementation of the ADNI and/or provided data but did not participate in the analysis or the writing of this report. A complete listing of the ADNI investigators can be found at: http://adni.loni.usc.edu/wp-content/uploads/how_to_apply/ADNI_Acknowledgement_List.pdf

Received 16 May 2015; revised 8 July 2015; accepted 18 July 2015; accepted article preview online 5 August 2015

INTRODUCTION

Late-onset Alzheimer's disease (AD, OMIM 104300, 104310) is the most common neurodegenerative disorder and leads to a progressive cognitive decline and dementia in the elderly (Alzheimer's Association, 2013; Querfurth and LaFerla, 2010). The major histological features of the disease include the presence of neurofibrillary tangles, extracellular amyloid β peptide (Aβ) deposition, synaptic dysfunction, and loss of neuronal integrity (Querfurth and LaFerla, 2010). The underlying cause of the disease is unclear in most cases, but numerous genetic alterations have been identified as being associated with Alzheimer's risk (Bertram *et al*, 2007; Karch and Goate, 2015; Lambert *et al*, 2013). Immune-related genes, especially complement genes such as complement receptor 1 (*CR1*) and clusterin (*CLU*; Bertram *et al*, 2007), have been identified as the top AD susceptibility genes

in European populations or of European origin, and the complement system has been reported to be involved in the initiation and development of AD (Crehan *et al*, 2012).

The complement regulator, Complement Factor H (*CFH*, OMIM 134370), has a key role in inhibiting complement activation and inflammation. *CFH* was recognized as the major genetic risk factor for age-related macular degeneration (AMD; Klein *et al*, 2005), which is another age-related neurodegenerative disease and shares similar risk factors and pathological features with AD (Sivak, 2013). CFH protein was suggested to be a potential top serum biomarker for AD (Hye *et al*, 2006, 2014; Thambisetty *et al*, 2008). However, the involvement of CFH in AD is contentious.

We performed a genetic screening in a Han Chinese cohort with AD for five immune genes (*CR1*, *CR2*, *CLU*, *CD33*, and *TREML2*) that were identified as the top AD susceptibility genes for Europeans (Bertram *et al*, 2007; Lambert *et al*, 2013). After the screening, a multiple-stage genetic association study focusing on the *CFH* gene was performed. We aimed to answer two key questions: (1) Do genetic variants in these immune genes, especially *CFH*, confer risk to AD in Han Chinese? and (2) How does CFH function in AD? The involvement of CFH in functional and structural brain changes, as well as AD biomarker (cerebrospinal fluid (CSF) tau and Aβ levels) alterations, were explored using data from the Alzheimer's Disease Neuroimaging Initiative (ADNI) project (Weiner *et al*, 2010). Moreover, the effect of AD-related *CFH* SNPs on morphological changes of hippocampus and entorhinal cortex, which were recognized as the most and the first affected regions of the brain with AD (Harris *et al*, 2010; Khan *et al*, 2014), respectively, was measured in healthy young adults at genetic risk by magnetic resonance imaging (MRI) scan. The effects of *CFH* genotypes and expression changes were analyzed in aged and AD brain tissues and in AD cellular models. Our collective data indicated that *CFH* is an important AD susceptibility gene and may affect the structure and function of the brain and alter the immune response as the disease progresses.

MATERIALS AND METHODS

Subjects

A two-stage cohort of 2041 Han Chinese with and without AD was analyzed. In stage 1, 380 patients (AD1, 45.8% men, mean age 76.5 ± 9.6 years, mean onset age 70.9 ± 9.7 years) and 475 healthy individuals from the general populations (PC1) were recruited from East China. In stage 2, we recruited 345 patients (AD2), 337 healthy individuals from the general populations (PC2), and 504 healthy longevity individuals (LC, age 93 ± 2.6 years; as another control) from Southwest China. Most of these AD patients had been analyzed for other risk loci in our recent studies (Bi *et al*, 2014, 2015; Wang *et al*, 2014). In brief, patients were diagnosed following the DSM-IV and the NINCDS-ADRDA criteria independently by at least two senior clinicians. The healthy controls were confirmed to have normal cognitive ability. Informed consents conforming to the tenets of the Declaration of Helsinki were obtained from all participants, or the supervisors of patients, after being given a complete description of the study. The institutional review board of the Kunming Institute of Zoology, Chinese Academy of Sciences, approved this study.

To confirm the results of the two-stage study, we performed jointed comparisons with multiple world-wide sample sets. Additional cohorts from East and Southwest China: 2460 individuals from Shanghai, 1549 individuals from Sichuan Province, and 2751 individuals from Yunnan Province (Zhang *et al*, 2014), which were enrolled for other genetic association analyses, were included in this analysis to enlarge the population controls. All of these subjects were collected from the general populations with normal cognitive ability and no history of dementia. Individuals with genotype data of rs800292 and rs1061170 available were included in our jointed comparison. Genetic data from ADNI (http://adni.loni.usc.edu/; Weiner *et al*, 2010) were also retrieved for re-analysis. Subjects with available genotype data from all stages of the ADNI 1/GO/2 were included in our analyses. These samples contain 760 individuals in the ADNI1 cohort (180 probable AD patients, 363 mild cognitive impairment (MCI) patients, and 214 cognitively normal aging controls) and 430 individuals in the ADNI GO/2 cohort (29 probable AD patients, 275 MCI patients, and 126 cognitively normal aging controls). Because of the limited sample size of probable AD, AD and MCI participants in these two cohorts were pooled as the patients' group. Previously reported data regarding the association of rs1061170 with AD (Hamilton *et al*, 2007; Le Fur *et al*, 2010; Proitsi *et al*, 2012; Zetterberg *et al*, 2008) were re-analyzed together with the data from our current samples. In total, 719 patients and 6217 population controls from China, and 845 patients and 345 controls of European origin were analyzed for rs800292; 713 patients and 6747 controls from China and 3604 patients and 10 048 controls of European origin were analyzed for rs1061170.

SNP Genotyping and Association Analysis

We genotyped 17 SNPs of five immune genes (*CR1*, *CR2*, *CLU*, *CD33*, and *TREML2*) that were identified as the top Alzheimer's susceptibility genes in Europeans (Bertram *et al*, 2007; Lambert *et al*, 2013) and 11 SNPs of the *CFH* gene in our stage 1 cohort from East China for the preliminary screening. Previously reported genome-wide association study (GWAS) top hits, tagging SNPs and potentially functional SNPs of these genes were selected for genotyping. The selection criteria and details for selected SNPs were described in the Supplementary Methods and Supplementary Table 1. *APOE* ε4 was determined as previously described (Bi *et al*, 2014, 2015; Wang *et al*, 2014).

Association analysis was carried out using PLINK (Purcell *et al*, 2007). Allelic (Table 1) and genotypic (Supplementary Table 2) comparisons with 2 d.f. genotypic, Cochran-Armitage trend, dominant, and recessive models were conducted for individual SNPs. All available samples from the general populations were pooled as a combined sample for Chinese (termed 'Combined Chinese', Table 2) and Europeans (termed 'Combined Europeans', Table 2), respectively. Comparison of the genotype counts between the combined case and control populations was estimated by the χ^2 test. Meta-analysis for the association of *CFH* SNPs with AD in the two combined sample sets was performed by using Review manager (RevMan 5.2, http://tech.cochrane.org/rev

Table 1 Association of *CFH* Variants with AD in Han Chinese Populations ($N = 20411$)

SNP	Allele	Stage 1 (SH:AD1 *vs* PC1)				Stage 2-1 (SC:AD2 *vs* PC2)				Stage 2-2 (SC:AD2 *vs* LC)			Combined (AD1+AD2 *vs* PC1+PC2)				
		F_{AD1}	F_{PC1}	OR (95%CI)	P_A	F_{AD2}	F_{PC2}	OR (95%CI)	P_A	F_{LC}	OR (95%CI)	P_A	F_{AD}	F_{PC}	OR (95%CI)	P_A	$P_{Corrected}$
rs800292	T/C	0.362	0.402	0.844 (0.693–1.028)	0.092	0.376	0.441	0.764 (0.615–0.949)	*0.015*	0.426	0.811 (0.664–0.989)	*0.038*	0.369	0.418	0.812 (0.702–0.940)	*5.1 × 10^{-3}*	*0.019*
rs1061170	C/T	0.066	0.039	1.749 (1.130–2.705)	*0.011*	0.073	0.043	1.749 (1.091–2.805)	*0.019*	0.037	2.047 (1.320–3.174)	*0.001*	0.069	0.041	1.759 (1.277–2.422)	*4.7 × 10^{-4}*	*0.005*
rs10801555	A/G	0.044	0.040	1.098 (0.682–1.769)	0.699	0.057	0.043	1.345 (0.822–2.201)	0.237	0.052	1.105 (0.721–1.693)	0.648	0.050	0.041	1.225 (0.871–1.722)	0.242	0.409
rs10922096	T/C	0.122	0.128	0.943 (0.706–1.260)	0.692	0.109	0.110	0.990 (0.704–1.393)	0.954	0.115	0.942 (0.691–1.284)	0.705	0.116	0.121	0.954 (0.765–1.189)	0.674	0.823
rs2019727	T/A	0.073	0.092	0.781 (0.549–1.110)	0.167	0.051	0.071	0.703 (0.449–1.102)	0.123	0.060	0.847 (0.552–1.300)	0.446	0.063	0.083	0.736 (0.558–0.971)	0.030	0.065
rs10733086	A/T	0.057	0.060	0.948 (0.630–1.425)	0.796	0.069	0.064	1.086 (0.708–1.666)	0.705	0.070	0.986 (0.672–1.446)	0.940	0.063	0.062	1.019 (0.759–1.367)	0.900	0.900
rs10737680	C/A	0.395	0.430	0.868 (0.715–1.055)	0.154	0.452	0.435	1.071 (0.865–1.327)	0.528	0.433	1.078 (0.887–1.311)	0.449	0.422	0.432	0.962 (0.833–1.110)	0.595	0.817
rs1410996	T/C	0.391	0.428	0.858 (0.706–1.042)	0.122	0.431	0.433	0.992 (0.800–1.230)	0.942	0.433	0.993 (0.816–1.208)	0.940	0.410	0.430	0.921 (0.797–1.063)	0.260	0.409
rs11582939	C/T	0.443	0.494	0.816 (0.673–0.988)	*0.037*	0.461	0.510	0.819 (0.662–1.013)	0.066	0.496	0.867 (0.714–1.054)	0.152	0.489	0.492	0.988 (0.857–1.138)	0.863	0.900
rs426736	T/C	0.532	0.458	1.345 (1.110–1.629)	*0.002*	0.494	0.503	0.965 (0.780–1.194)	0.745	0.489	1.021 (0.840–1.240)	0.836	0.520	0.474	1.199 (1.040–1.382)	*0.012*	*0.034*

Abbreviations: AD1, patients with AD of stage 1 from Shanghai (SH); AD2, patients with AD of stage 2 from Sichuan (SC); CI, confidence interval; F_x, minor allele frequency of the 'x' population; LC, longevity controls of stage 2 from Sichuan; OR, odds ratio; P_A, allelic association *P*-value; $P_{Corrected}$, adjusted *P*-value (combined P_A) for multiple testing by Benjamini-Hochberg FDR (FDR_BH) control algorithm; PC1, population controls of stage 1 from Shanghai; PC2, population controls of stage 2 from Sichuan. The *P*-values less than 0.05 were marked in italic. Results of genotypic associations and genotype counts distribution were shown in Supplementary Table 2.

man), with the Cochran–Mantel–Haenszel method under a fixed effect. The heterogeneity was measured by the I^2 index (Higgins and Thompson, 2002; Table 2).

The genetic associations were explored further by estimating the significance of SNP–SNP interaction using the multifactor-dimensionality reduction (MDR) method (Ritchie *et al*, 2001) or the '—epistasis' command in PLINK (Purcell *et al*, 2007).

Neuroimaging Analysis for the Effects of CFH Variants on Structural and Functional Brain Changes

We recruited 360 healthy young adults (age 19.4 ± 1.1 years; 51.7% men) to study the effects of the Alzheimer's risk *CFH* SNPs on morphological changes of the brain. These samples were described in our previous study and were effective to identify risk alleles affecting brain structure variations (Li *et al*, 2015; Zhang *et al*, 2015). MRI scans were performed on a MR750 3.0 Tesla magnetic resonance scanner (GE Healthcare, detailed parameters in Supplementary Methods). The protocol was approved by the Ethics Committee of School of Life Science and Technology at University of Electronic Science and Technology of China.

First, we performed a whole-brain voxel-based morphometry analysis for volume and density of the gray matter. Second, we detected the effect of the AD-risk *CFH* SNPs on total intracranial volume (ICV) and hippocampus volume changes. Finally, we tested the effect of the AD-risk *CFH* SNPs on the thickness of the entorhinal cortex. To test the effect of *CFH* genotypes on brain morphological changes, we applied a general linear regression model adjusted for gender, age, education year, and ICV. To correct for multiple comparisons for the entorhinal cortex, the statistical significance level was set as $P < 0.005$ (0.05/10 [5 SNPs × 2 hemisphere], Bonferroni correction). Details regarding the imaging process and statistics were described in Supplementary Methods.

Detecting the Effects of AD-Risk SNPs on AD Endophenotypes

To confirm our results and investigate further the role of CFH in AD pathogenesis, we obtained genetic, neuroimaging, and biomarker data from the ADNI project (http://adni.loni.usc.edu/; Weiner *et al*, 2010). Effect of the top AD-risk *CFH* SNP (only rs800292 was available) on AD endophenotypes, eg, CSF tau and Aβ levels, cognitive score, entorhinal regional atrophy rate, and entorhinal volume, was analyzed using PLINK (Purcell *et al*, 2007).

Expression Quantitative Trait Loci (eQTL) Analysis

To investigate the effect of *CFH* variants on *CFH* mRNA expression level, we performed eQTL analysis in 10 brain regions of 134 neuropathologically normal individuals. Details were shown in Supplementary File and the brain eQTL database (http://www.braineac.org/; Ramasamy *et al*, 2014). The eQTL effect of the *CFH* variants was validated by using the Genotype-Tissue Expression project (GTEx, http://www.gtexportal.org/home/) database, which provides a comprehensive atlas of gene expression and regulation across multiple human tissues (The GTEx

Table 2 Validating the Associations of rs800292 and rs1061170 with AD in Enlarged Sample Sets

SNP	Population	Case		Control		*P*-value	OR
		N	MAF	*N*	MAF		
rs800292	Shanghai[a]	377	0.362	1917	0.410	1.6×10^{-2}	0.82
	Sichuan[b]	342	0.376	1549	0.419	3.7×10^{-2}	0.84
	Combined[c]	719	0.369	3466	0.414	2.0×10^{-3}	0.83
	Combined Chinese[d]	719	0.369	6217	0.415	7.0×10^{-4}	0.82
	ADNI_1[e]	543	0.236	214	0.304	6.0×10^{-3}	0.71
	ADNI_GO2[e]	302	0.207	126	0.246	2.1×10^{-1}	0.78
	European (ADNI)	845	0.225	340	0.282	3.0×10^{-3}	0.74
	Meta-analysis[f]	1564	—	6557	—	1.3×10^{-5}	0.80
rs1061170	Shanghai[a]	377	0.066	2460	0.055	2.2×10^{-1}	1.21
	Sichuan[b]	336	0.073	1542	0.043	3.0×10^{-3}	1.65
	Combined[c]	713	0.069	4002	0.051	6.0×10^{-3}	1.38
	Combined Chinese[d]	713	0.069	6747	0.057	5.5×10^{-2}	1.24
	European (Zetterberg *et al*, 2008)	800	0.427	1265	0.394	3.9×10^{-2}	1.14
	European (Le Fur *et al*, 2010)	701	0.357	6990	0.361	7.7×10^{-1}	0.98
	European (Proitsi *et al*, 2012)	2103	0.385	1793	0.375	3.4×10^{-1}	1.05
	Combined Europeans[g]	3604	0.389	10048	0.368	1.0×10^{-3}	1.09
	Meta-analysis[h]	4317	—	16795	—	5.0×10^{-4}	1.10

Abbreviation: MAF, minor allele frequency.
[a]Enlarged general population controls including the case-matched controls and available general individuals with normal cognitive ability from Shanghai (author's unpublished data).
[b]Enlarged controls including the case-matched controls and other available general individuals with normal cognitive ability from Sichuan (author's unpublished data).
[c]Samples combining both Shanghai and Sichuan subjects.
[d]Chinese samples combining Shanghai, Sichuan, and Yunnan subjects with available genotype data as the general population control. For rs800292: heterogeneity among combined Chinese populations, $\chi^2 = 0.03$, d.f. = 1 ($P = 0.86$), $I^2 = 0\%$, overall meta-analysis effect $Z = 3.21$ ($P = 0.001$). For rs1061170: heterogeneity among combined Chinese populations, $\chi^2 = 2.34$, d.f. = 1 ($P = 0.13$), $I^2 = 57\%$, overall meta-analysis effect $Z = 3.05$ ($P = 0.002$).
[e]Data retrieved from the ADNI (Alzheimer's Disease Neuroimaging Initiative) project. For rs800292: heterogeneity among combined European populations, $\chi^2 = 0.32$, d.f. = 1 ($P = 0.57$), $I^2 = 0\%$, overall meta-analysis effect $Z = 2.95$ ($P = 0.003$); genotype data of rs1061170 is not available in the ADNI subjects.
[f]Meta-analysis for rs800292 in combined Chinese and Europeans; heterogeneity: $\chi^2 = 0.91$, d.f. = 1 ($P = 0.34$), $I^2 = 0\%$; overall meta-analysis effect $Z = 4.32$ ($P < 0.0001$).
[g]All three available European sample sets were pooled together as a combined European population, with the original genotype counts measured by χ^2 test; heterogeneity among populations, $\chi^2 = 3.04$, d.f. = 2 ($P = 0.22$), $I^2 = 34\%$, overall meta-analysis effect $Z = 1.48$ ($P = 0.14$).
[h]Meta-analysis for rs1061170 in combined Chinese and Europeans, heterogeneity: $\chi^2 = 0.93$, d.f. = 1 ($P = 0.34$), $I^2 = 0\%$, overall effect $Z = 3.49$ ($P = 0.0005$). The *P*-values less than 0.05 were marked in italic.

Consortium, 2013). The tibial nerve tissue ($n = 102$) was used in the analysis; the other brain tissues, such as cortex or hippocampus, had a sample size less than 30 and was not considered (http://www.gtexportal.org/home/). For the effect of the *CFH* variants on CFH protein level, we used an earlier GWAS data of plasma CFH levels (Ansari *et al*, 2013).

CFH mRNA Expression Alterations in Aged and AD Brains and AD Cellular Models

A total of 49 hippocampal samples of *Rattus norvegicus* at 5 age points (3, 6, 9, 12, and 23 months, GSE9990; Kadish *et al*, 2009) and 30 postmortem frontal cortex of normal individuals at 26–106 years of age (GSE1572; Lu *et al*, 2004) were used to assess *CFH* mRNA expression changes during brain aging. Expression data of 272 human postmortem dorsolateral prefrontal cortex (DLPFC) of normal subjects across the lifespan from the BrainCloud (http://braincloud.jhmi.edu/; Colantuoni *et al*, 2011) were also included to investigate the expression pattern of *CFH* with aging. In all, 22 hippocampal samples from postmortems showing AD at different stages of severity (GSE1297; Blalock *et al*, 2004), and entorhinal cortex neurons containing neurofibrillary tangles from 10 mid-stage patients (GSE4757; Dunckley *et al*, 2006) were used to assess *CFH* mRNA expression changes during disease processing. Expression differences between groups were measured by Student's *t*-test using GraphPad Prism 5.0 (GraphPad Software, Inc., La Jolla, USA). The expression data were retrieved through the Gene Expression Omnibus (GEO, http://www.ncbi.nlm.nih.gov/sites/GDSbrowser). Correlation analysis was performed for the mRNA expression of *CFH* and *APP* in hippocampus of AD patients (GSE1297; Blalock *et al*, 2004).

U251 cells (a glioma cell line) with $A\beta_{1-42}$ treatment or with stable overexpression of APP mutant (APP^{Mut}, APP-p.M671L) and PSEN1 mutant ($PSEN1^{Mut}$, PSEN1-p.M139V/M146L/H163R) were used as AD cellular models to test *CFH* expression changes in response to these stimuli. Quantitative real-time PCR was used to determine the relative mRNA level of the *CFH* gene in the AD cellular models. Detailed information was shown in the Supplementary Materials.

RESULTS

Genetic Screening of the AD-Related Immune Genes and CFH in Han Chinese Patients with AD

SNPs within the five AD-related top immune genes (*CR1*, *CR2*, *CLU*, *CD33*, and *TREML2*) identified in Europeans showed no association with AD in our stage 1 Chinese samples (Supplementary Table 1). We observed positive associations of *CFH* SNPs rs426736 (OR = 1.345, allelic $P = 2.4 \times 10^{-3}$, genotypic $P = 1.2 \times 10^{-2}$) and rs1061170 (p.Y402H, OR = 1.749, allelic $P = 1.1 \times 10^{-2}$, genotypic $P = 1.3 \times 10^{-2}$) with AD, whereas rs800292 (p.V62I) and rs11582939 showed a marginal significance (Table 1 and Supplementary Table 2) in our stage 1 samples.

We replicated the association of *CFH* with AD in stage 2 cohort. Associations of both rs1061170 (OR = 1.749, allelic $P = 1.9 \times 10^{-2}$, genotypic $P = 3.4 \times 10^{-2}$) and rs800292 (OR = 0.764, allelic $P = 1.5 \times 10^{-2}$, genotypic $P = 6.5 \times 10^{-4}$) with AD were confirmed. When the cases were compared with the healthy longevity controls (>90 years old), rs1061170 (OR = 2.047, allelic $P = 1.1 \times 10^{-3}$, genotypic $P = 9.3 \times 10^{-4}$) showed a much stronger association with AD, and the association of rs800292 (OR = 0.811, allelic $P = 0.038$, genotypic $P = 3.0 \times 10^{-3}$) with AD remained significant. We combined the two independent samples and found that rs1061170 (OR = 1.759, $P_{\mathrm{FDR\_BH}} = 5.2 \times 10^{-3}$) and rs800292 (OR = 0.812, $P_{\mathrm{FDR\_BH}} = 1.9 \times 10^{-2}$) showed strong associations even after correcting for multiple testing (false discovery rate (Benjamini Hochberg), FDR_BH). No SNP–SNP interaction among *CFH* variants and between *CFH* and *APOE* SNPs (rs429358 and rs7412 that defining the $\epsilon 4$ status) was observed, suggesting that *CFH* was involved in AD independently of *APOE*.

Validating the Association of CFH with AD in the Enlarged Sample Sets

We validated the association of the most robust *CFH* SNPs rs800292 and rs1061170 with AD in enlarged world-wide sample sets (Table 2). Compared with the pooled larger population controls ($n = 3466$) from East and Southwest China, the association of rs800292 with AD remained robust ($P = 2.0 \times 10^{-3}$). When all the population controls ($n = 6217$) were considered, the association was even stronger ($P = 7.0 \times 10^{-4}$). Analysis of the ADNI data showed that rs800292 was also associated with AD in Europeans (845 cases *vs* 340 controls; $P = 3.0 \times 10^{-3}$). Meta-analysis combining all Chinese and European samples (1564 cases *vs* 6557 controls), which would increase the statistical power and had no significant study heterogeneity (cf. the footnote of Table 2), further validated the association of rs800292 with AD ($P_{meta} = 1.3 \times 10^{-5}$, OR = 0.80).

Similarly, we validated the association of rs1061170 with AD in combined population controls ($n = 4002$) from East and Southwest China ($P = 6.0 \times 10^{-3}$), but this effect turned out to be marginally significant ($P = 5.5 \times 10^{-2}$) when all Han Chinese controls ($n = 6747$) were considered. Combined analysis of previously reported data showed a positive association of rs1061170 with AD in Europeans (3604 cases *vs* 10048 controls; $P = 1.0 \times 10^{-3}$). When all combined Han Chinese and European samples (4317 cases *vs* 16795 controls) were used for meta-analysis, we observed a significant association between rs1061170 and AD ($P_{meta} = 5.0 \times 10^{-4}$, OR = 1.10; Table 2).

Effects of the AD-Risk CFH SNPs on Structural Brain Changes in Young Adults

We detected the effects of the AD-risk *CFH* SNPs on morphological changes of the brain in young individuals using structural MRI scan. The AD-related *CFH* SNPs had no apparent effect on estimated total ICV (Supplementary Figure 2) and hippocampal volume (Figure 1 and Supplementary Table 3) in our pilot screening. However, all suggestive AD-associated *CFH* SNPs showed a trend of association with the entorhinal thickness (Supplementary Table 4). Both rs1061170 ($P = 2.5 \times 10^{-3}$) and rs800292 ($P = 4.7 \times 10^{-4}$) were significantly associated with the entorhinal thickness, especially for the right entorhinal cortex (Figure 1). Intriguingly, the AD-risk allele carriers have increased thickness of the entorhinal cortex in the right hemispheres (Figure 1) in their early age. It was reported that trans-synaptic progression of Aβ-induced cortex dysfunction and cortical spread was driven and initiated from the entorhinal cortex in preclinical Alzheimer's disease (Harris *et al*, 2010; Khan *et al*, 2014). Interference of the entorhinal cortex may contribute to the development of AD.

Effects of the AD-Risk CFH SNPs on AD Endophenotypes and CFH Expression

Our MRI scan analyses showed that individuals at risk of AD had a thicker entorhinal cortex in early life, suggesting a potential compensatory effect. Indeed, we observed a decreased volume of the entorhinal cortex in AD patients with risk allele of rs800292 (Figure 2g, h), indicating a higher atrophy rate of risk allele carriers as confirmed in our regional atrophy rate analysis (Figure 2i). In addition, risk allele carriers of rs800292 showed a marginally significant ($P < 0.05$) decrease of cognitive score (Figure 2j), and increase of CSF tau (Figure 2k) and Aβ (Figure 2l) levels. These observations added more support for the contribution of *CFH* variants to AD susceptibility and development. Note that we also found a positive association of *CFH* variant with MCI patients using the ANDI data (Supplementary Table 5), which suggested that an analysis for the association between AD stage and *CFH* genotype might be rewarding.

Besides their effects on AD neuroimaging and biomarker endophenotypes, the risk alleles of rs800292 and rs1061170 were associated with lower *CFH* mRNA level (Figure 2). In particular, the *CFH* mRNA level was significantly decreased in the inferior olivary nucleus (MEDU, $P < 0.01$) and occipital cortex (OCTX, $P < 0.05$) in carriers with the risk allele C of rs1061170 (Figure 2a–c). The most significant genotype-affected *CFH* mRNA changes were observed for an exon-specific probe 2373392, which showed strong associations in all 10 brain regions (aveALL, $P < 0.001$, Figure 2d) and hippocampus (HIPP, $P < 0.01$, Figure 2e). In addition, carriers of rs800292 risk allele showed a significantly decreased *CFH* mRNA expression level in MEDU (Figure 2f). The significant decrease of *CFH* mRNA level associated with rs800292 and rs1061170 risk alleles could be validated in the tibial nerve tissues using the GTEx data (Supplementary Figure 3). Note that our results were in

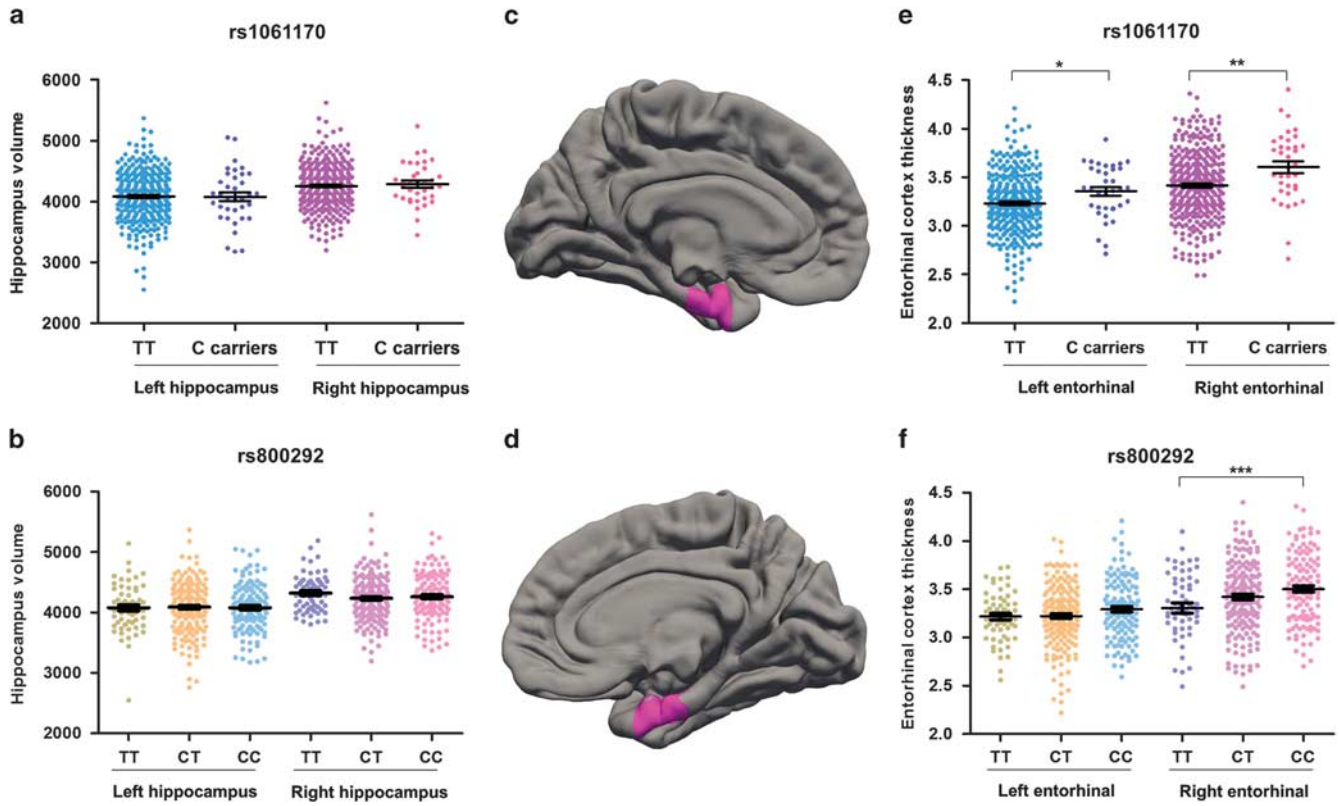

Figure 1 Risk allele carriers have similar hippocampal volume and thicker entorhinal cortex compared with non-risk allele carriers at young age. Regression analysis was conducted to detect the associations of rs1061170 (Y402H) and rs800292 (V62I) with bilateral hippocampal volume (a and b) and entorhinal cortical thickness (e and f). The left entorhinal cortex (c) and the right entorhinal cortex (d) were labeled in FreeSurfer. *$P<0.05$, ** $P<0.01$, ***$P<0.001$, linear regression analyses. Data represent mean ± SEM.

agreement with a reported GWAS study showing a significant association of lower serum CFH protein level with the AD-risk allele of rs1061170 (Ansari *et al*, 2013).

CFH mRNA Expression in Aged and Alzheimer's Brain Tissues and Cellular Assays

As we have observed a decrease of CFH expression levels in risk allele carriers, we further evaluated the alteration of *CFH* mRNA expression in aged and AD brains and AD cellular models. There was an increase of *Cfh* mRNA level with age in the rat hippocampus (Figure 3a). A similar pattern of upregulated *CFH* mRNA during aging was observed in human frontal cortex samples from 30 normal individuals of age 26–106 years (Figure 3b). The significant increase of *CFH* expression level with aging was confirmed in human prefrontal cortex using the BrainCloud data (Supplementary Figure 4). Moreover, *CFH* mRNA expression level increased in hippocampus as the severity of the disease worsened (Figure 3c). We also observed an increase of *CFH* mRNA level in entorhinal neurons containing neurofibrillary tangles compared with normal neurons, although the increase was not significant. The expression of C3, the central component of the complement system, was strongly elevated in tangled entorhinal neurons (Figure 3d). Considering its anti-inflammatory role, the increase of CFH may be the result of aging and balanced CFH level may have a protective effect on aging.

In $A\beta_{1-42}$-treated U251 cells, we observed a significant increase of *CFH* mRNA level (Figure 3f). Expression level of *CFH* was also increased in cells with stable overexpression of APP mutant (APP^{Mut}, APP-p.M671L) and PSEN1 mutant ($PSEN1^{Mut}$, PSEN1-p.M139V/M146L/H163R; Figure 3h). Consistent with the results of cellular assays, *CFH* mRNA level was positively correlated with *APP* mRNA level in hippocampus of AD patients (Pearson $R^2=0.41$, $P=0.007$; Figure 3e). This significant correlation disappeared in control sample or patient–control combined sample (Supplementary Figure 5). Taken together, our results indicated a protective role of increased CFH level in brain aging and AD development, whereas the *CFH* risk alleles were associated with lower CFH level, resulting in an insufficient protection of this immune regulator.

DISCUSSION

Increased activity of the complement system has been reported to be involved in the initiation and development of AD (Crehan *et al*, 2012). Immune genes, especially complement genes, were identified as the top Alzheimer's susceptibility genes in Europeans (Bertram *et al*, 2007; Lambert *et al*, 2013). However, our analysis showed that these genes (*CR1*, *CLU*, *CD33*, and *TREML2*) had very weak effects in Han Chinese. Intriguingly, we found that *CFH*, the most important genetic factor for AMD (Klein *et al*, 2005),

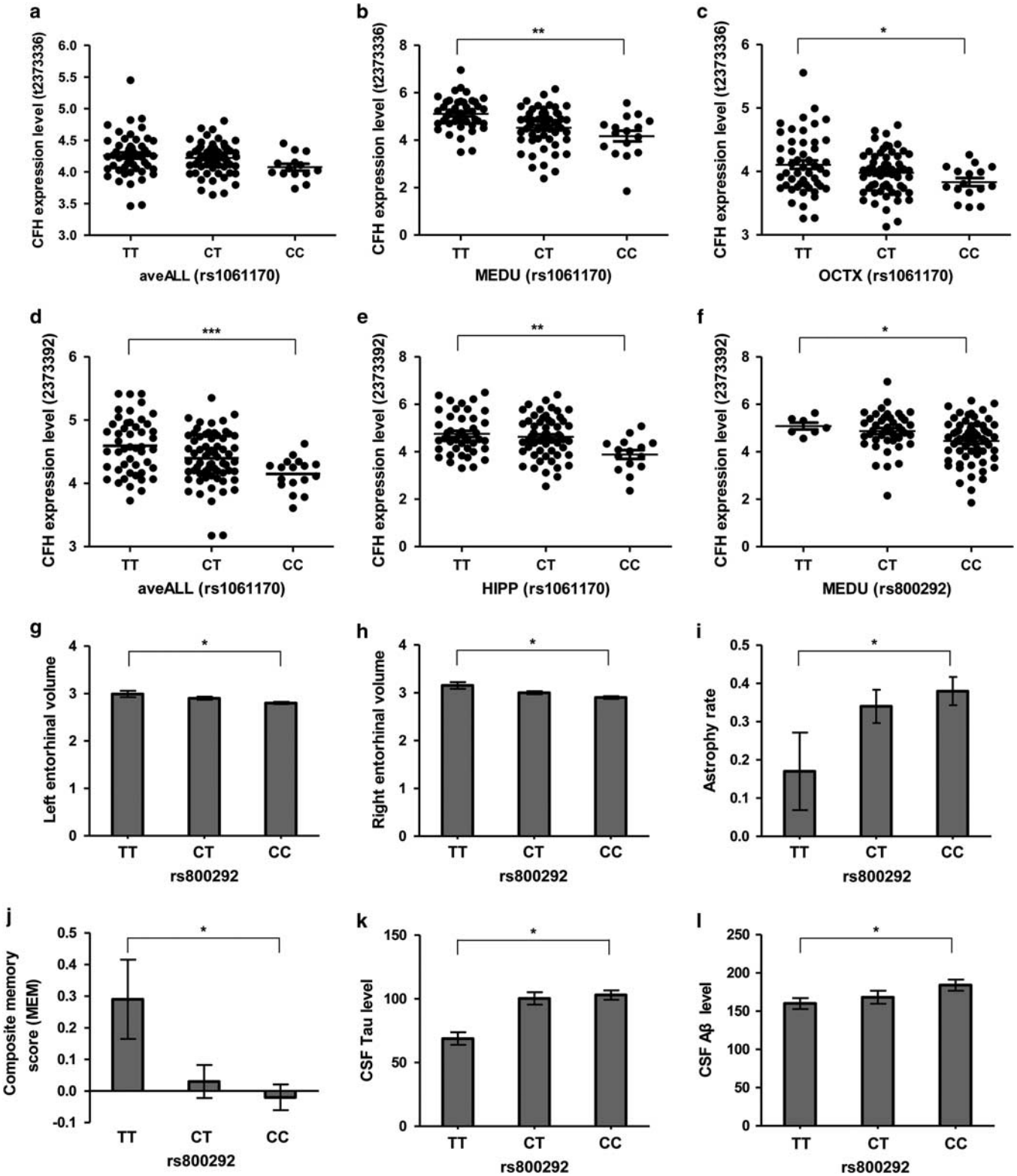

Figure 2 Effects of AD-risk *CFH* SNPs on *CFH* expression and AD endophenotypes. eQTL effect of AD-risk *CFH* SNPs (rs1061170 and rs800292) on *CFH* mRNA expression level was investigated in brain tissues using Affymetrix Human Exon 1.0 ST Array data from the UK Brain Expression Consortium (UKBEC; Ramasamy *et al*, 2014). We retrieved the genotyping and expression data from the UKBEC web server (http://www.braineac.org/; Ramasamy *et al*, 2014). Affymetrix ID t2373336 (a–c), *CFH* transcript probe; Affymetrix ID 2373392 (d–f), *CFH* exon-specific probe (chr1: 196712667–196712698). aveALL, average expression level among the 10 available brain regions; MEDU, the inferior olivary nucleus (sub-dissected from the medulla); OCTX, occipital cortex; HIPP, hippocampus. The potential effects of AD-risk *CFH* SNP rs800292 on AD-related endophenotypes, eg, entorhinal volume (g–h), entorhinal regional atrophy rate (i), composite memory score (MEM, j), and CSF tau (k) and Aβ (l) levels, were analyzed using data retrieved from the ADNI project (http://adni.loni.usc.edu/; Weiner *et al*, 2010). Data represent mean ± SEM. $^{*}P<0.05$, $^{**}P<0.01$, $^{***}P<0.001$, one-way ANOVA for eQTL analysis; linear regression analyses for SNP rs800292 on AD-related endophenotypes.

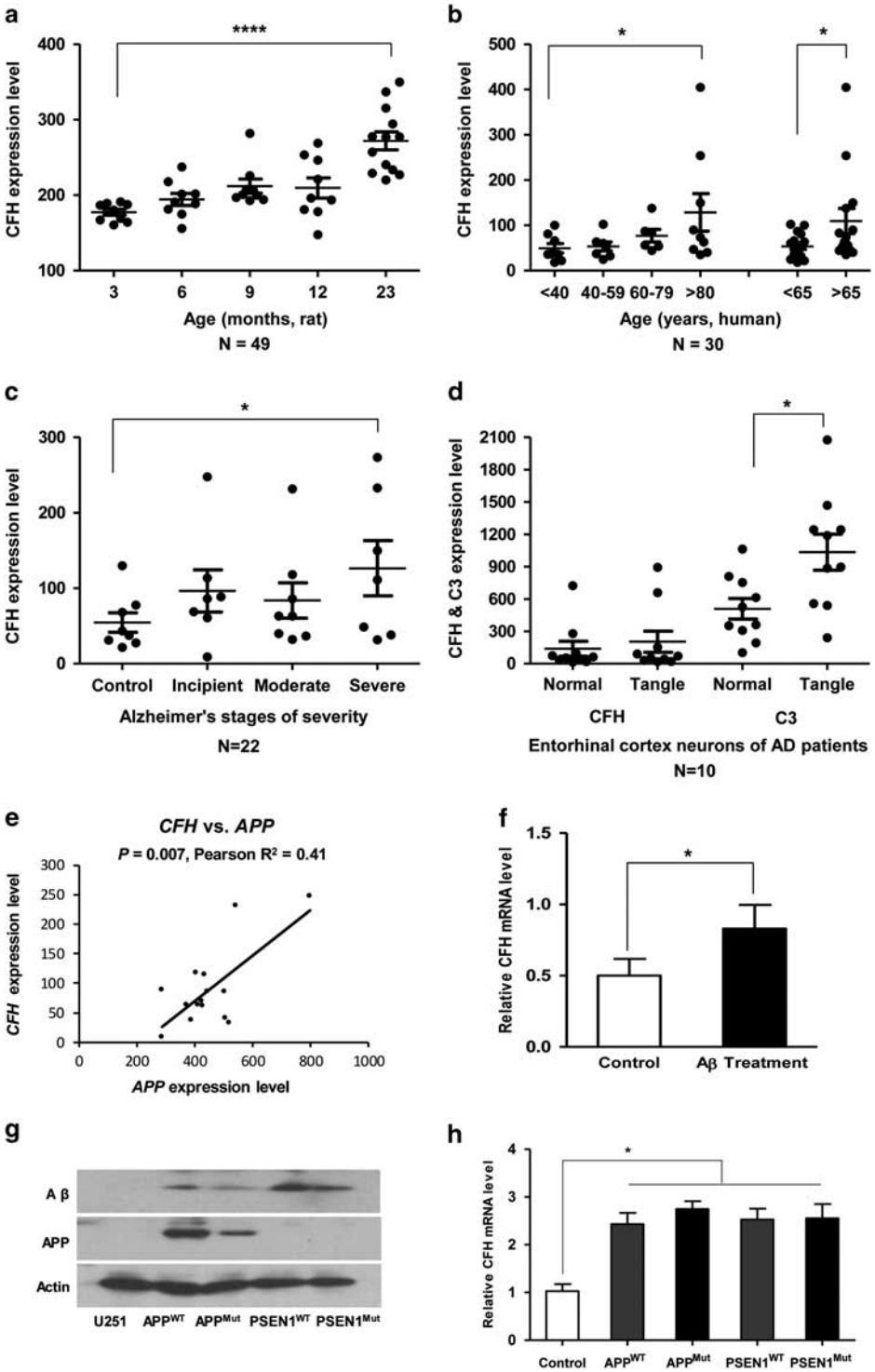

Figure 3 *CFH* expression in aged and AD brains and cellular assays. (a) *Cfh* mRNA expression changes in the hippocampus from 49 *Rattus norvegicus* across the adult lifespan. (b) *CFH* mRNA expression of the postmortem frontal cortex from 30 normal individuals from 26 to 106 years of age. (c) *CFH* mRNA expression in brain hippocampus from 22 postmortem subjects with AD at different stages of severity. (d) *CFH* and *C3* mRNA expression levels in entorhinal cortex neurons containing neurofibrillary tangles were increased relative to those of normal neurons from the same brain region in 10 mid-stage AD patients. (e) Correlation between *CFH* mRNA level (213800_at) and *APP* mRNA level (probe 211277_x_at) in hippocampus of AD patients ($N = 15$) with incipient and moderate stages of severity. (f) Increase of *CFH* mRNA expression in U251 cells with $A\beta_{1-42}$ treatment. (g) The APP and Aβ levels in cells with stable overexpression of APP (wild-type (APP^{wt}) and APP-p.M671L mutant (APP^{Mut})) and PSEN1 (wild-type ($PSEN1^{wt}$) and PSEN1-p.M139V/M146L/H163R ($PSEN1^{Mut}$). (h) *CFH* mRNA expression level was increased in cells with stable overexpression of APP and PSEN1. Data represent mean ± SEM. $^{*}P < 0.05$, $^{****}P < 0.0001$, Student's *t*-test.

acts as an important AD susceptibility gene in Han Chinese patients and has multiple roles in AD pathology.

CFH Variants are Associated with Brain Changes and Confer Alzheimer's Susceptibility

By a comprehensive analysis of the *CFH* SNPs in Han Chinese with and without AD, and a meta-analysis of world-wide published data, we found that several SNPs, especially rs1061170 (a well-known causal risk SNP for AMD; Klein *et al*, 2005) and rs800292, showed robust associations with AD (Table 1). This result clarified the previous conflicting observations (Hamilton *et al*, 2007; Le Fur *et al*, 2010; Proitsi *et al*, 2012; Zetterberg *et al*, 2008). It is to be noted the risk allele C of rs1061170 presents with a marked regional distribution (7% in the East Asian Ancestry population, 28% in the African Ancestry population, 41% in the European Ancestry population; data from the 1000 genome (http://www.1000genomes.org; Abecasis *et al*, 2012) and this might account for the different patterns of association between different populations. The higher risk allele frequency in Europeans might interpret partially the higher prevalence of AMD (Wong *et al*, 2014) and AD (cf. Alzheimer's Disease International, World Alzheimer Report 2009: The Global Prevalence of Dementia, http://www.alz.co.uk/research/world-report-2009) in Europeans than in Asians, although the effect size of the risk allele was smaller in Europeans than in Asians.

Intriguingly, our neuroimaging analysis showed that the Alzheimer's risk alleles were associated with an increased right entorhinal thickness in young adults (Figure 1). The brain immune cell glia, the most abundant cells in brain, was previously reported to contribute to half of brain volume changes and would be overactive in neuro-inflammation (DiBattista *et al*, 2014). It is thus possible that the increase in entorhinal cortex thickness might be due to a deficit in *CFH* risk allele carriers to control neuro-inflammation in the brain, as CFH serves an anti-inflammatory component. In addition, it has been reported that increased entorhinal cortex volume during the brain development could indicate a deficit in neural efficiency (DiBattista *et al*, 2014; Gogtay *et al*, 2004). Although the molecular and cellular mechanisms responsible for the increased entorhinal thickness in young *CFH* risk allele carriers remained to be elucidated, this result is not unexpected as the entorhinal cortex has an essential role in AD (Khan *et al*, 2014). There are further lines of evidence supporting an enhanced entorhinal structure or activity in healthy adults with young age and a higher atrophy rate as the disease progresses for those risk allele carriers. For instance, healthy *APOE* ε4 carriers showed a thicker right entorhinal cortex as compared with the left hemisphere (Donix *et al*, 2013) and a thinner left entorhinal cortex in *APOE* ε4 carriers than in non-carriers could be identified in children and adolescents (Shaw *et al*, 2007). Meanwhile, *APOE* ε4 may lead to an increased activity but greater atrophy in right hemisphere in healthy young subjects (O'Dwyer *et al*, 2012). The Alzheimer's risk *BDNF* genotype (Val/Val of Val66Met) carriers had a thicker entorhinal thickness in early adult life and a higher rate of entorhinal atrophy in elderly (Voineskos *et al*, 2011). These observations indicated that young healthy individuals at risk may have altered entorhinal thickness and improved brain activity. It might reflect a compensatory hypothesis (Filippini *et al*, 2009) wherein disease risk individuals appear to require additional effort to achieve comparable performance levels to overcome potential preclinical neural dysfunction.

Indeed, our data showed that AD-related *CFH* variant rs800292 not only altered the brain structure (eg, entorhinal cortex) in early life, but also affected the atrophy rate of the entorhinal cortex, CSF tau and Aβ levels, and memory decline as the disease progresses (Figure 2). These results suggest that *CFH* is actively involved in the onset and development of AD by promoting structural and functional brain changes. These observations indicated a role of immune genes in neuroimaging alterations in early age.

Alteration of CFH Expression is Involved in AD

Consistent with previous reports that CFH protein has the potential to be a biomarker for AD (Hye *et al*, 2006, 2014) and the above genetic association results, we found that *CFH* mRNA level in the hippocampus increases with age, suggesting an active role of CFH in the brain aging process (Figure 3). Moreover, there was a positive correlation between *CFH* mRNA level and severity of AD (and APP mRNA level) in brain tissues, and this result was consistent with the previous finding of increased CFH protein in the AD brain (Honda *et al*, 2000; Strohmeyer *et al*, 2000, 2002). Note that there are some controversies regarding serum CFH level in AD: an increase of CFH level was observed in the serum of AD patients (Hye *et al*, 2006, 2014); however, serum CFH level was reported to be significantly down-regulated in patients with AD and mild cognitive impairment (Gezen-Ak *et al*, 2013). The exact reason for this discrepancy remains unknown. Based on our results, we speculate that higher brain CFH levels may be related to AD development, supported by the observed increase of *CFH* mRNA levels in our cellular assays in response to $A\beta_{1-42}$ treatment or with stable overexpression of APP mutant and PSEN1 mutant (Figure 3).

Implications of CFH in the Pathogenesis of AD

Recent studies have demonstrated that the risk allele 402H (allele C of rs1061170) interacts less well (compared with 402Y (allele T)) with the binding sites in CFH ligands within the macula, resulting in complement activation and inflammation that may contribute to the accumulation of drusen, thus leading to the initiation and progression of AMD (Clark *et al*, 2010). There may be a similar mechanism by which Y402H may contribute to progression of AD. It is now known that Aβ plaques and local inflammation are central to the pathogenesis of AD (Kamer, 2010; Wyss-Coray, 2006). In addition to the anti-inflammation role, CFH acts as an extracellular matrix component and interacts with a wide selection of ligands (Ferreira *et al*, 2010), such as the C-reactive protein (Strang *et al*, 2012), heparin (Bergamaschini *et al*, 2009), zinc (Suh *et al*, 2000), and sialic acid (Patel *et al*, 2006). All these ligands may be involved in the accumulation of senile plaque in the AD brain. It has been reported that the risk allele 402H presented a reduced affinity to these ligands (Ormsby *et al*, 2008). Hence, patients harboring risk allele 402H might bind less CFH in amyloid

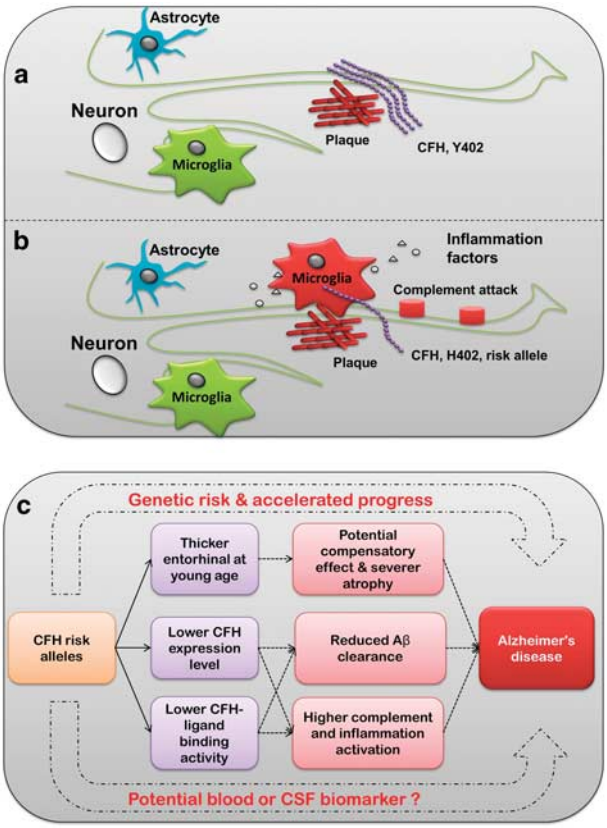

Figure 4 A simplified schematic profile for modeling the effect of CFH in AD. CFH acts as an extracellular matrix component and interacts with a wide range of ligands. The Alzheimer's risk allele 402H (rs1061170 C) was associated with lower CFH expression level and activity, thus presents a reduced affinity for these ligands. Patients harboring the risk allele 402H (b) may bind less CFH in the Aβ plaque compared with the wild-type (a), resulting in impaired regulation of complement activation (eg, membrane attack complex) and chronic local inflammation (inflammatory recruitment) in 402H carriers, which finally contributes to the accumulation of deposits and neuron loss during the development of AD. (c) Summary of the potential role of CFH in AD pathogenesis.

plaques, resulting in an impaired regulation of complement activation and local inflammation that may contribute to the accumulation of deposits and neuron loss in the development of AD (Figure 4). Furthermore, patients harboring the risk allele 402H might have decreased CFH levels in their brains according to our eQTL analysis. With impaired CFH levels and activity, extracellular deposition in the nidus may lead to inappropriate complement activation and thus contribute to the progression of clinical disease (Figure 4). Plaques in the AD brain, drusen in the eyes of patients with AMD, drusen-like deposits in the kidney of patients with kidney diseases, and even in the arteries of patients with atherosclerosis may also be the result of such processes. Further *in vivo* experiments using AD animal models are warranted to confirm our speculation.

It is worth mentioning that *CFH* was identified as the most important genetic factor for AMD (Klein *et al*, 2005) and its SNPs associated with AD were found to be risk SNPs for AMD; are we really bringing these two diseases, which share similar pathological characteristics and environmental risk factors (Keenan *et al*, 2014; Sivak, 2013), much closer based on this study? Significant cognitive impairment and subsequent occurrence of AD in AMD patients have been reported (Baker *et al*, 2009; Kaarniranta *et al*, 2011; Pham *et al*, 2006; Sivak, 2013; Woo *et al*, 2012), although the conclusion remains controversial (Kaarniranta *et al*, 2011; Keenan *et al*, 2014). The sequential occurrence of brain and retinal damage needs to be clarified. Our current observations added more evidence to the notion that AMD and AD, to some extent, share some common pathological features such as chronic oxidative stress and inflammation, active complement involvement, and intra- and extracellular deposits (Kaarniranta *et al*, 2011). These two diseases likely represent two related but distinct parallel amyloidopathies that might benefit from common targeted therapeutic approaches.

The presence of the *CFH* risk alleles in AD and AMD poses an evolutionary paradox during human evolution, as the diseases may have negative effects on fitness, but the risk alleles have not been eliminated by natural selection and persist within global populations. Why the deleterious allele 402H (rs1061170 C) was retained in populations with a relatively high frequency? We performed a positive selection analysis on the *CFH* region to look for an evolutionary explanation of this phenomenon. Two online tools for detecting positive selection in human genome were used: Haplotter (Voight *et al*, 2006; using the HapMap data) and CMS viewer (http://www.broadinstitute.org/mpg/cmsviewer/, using the 1000 genome data; Supplementary Figure 6). Positive selection was observed in a region next to the *CFH* gene cluster in African and Asian populations, which contains the *ASPM* (abnormal spindle-like microcephaly associated) gene. This gene controls brain development and was reported to have evolved rapidly in human (Zhang, 2003). However, it is the *CFH* region itself that showed evidence of positive selection in the European (CEU) population, consistent with the fact that the CEU population also has a higher prevalence of AD and AMD. These observations indicate an evolutionary imprint on this region that may affect AD. The risk allele 402H may provide an advantageous effect against pathogens, which can evade complement attack by recruitment of CFH (Ferreira *et al*, 2010). Therefore, it is possible that the derived 402H allele was retained during evolution to limit immune evasion by potential pathogens. Because of this trade-off effect, the retained allele may contribute a deleterious effect on common diseases (such as AMD, AD, uremia, and atherosis), which commonly affect the elderly in our modern world.

In summary, our results showed that *CFH* may contribute to AD development by affecting neuroimaging endophenotypes and biomarkers as well as immune response. Most of all, *CFH* affects structural change of the entorhinal cortex in early life and atrophy rate during AD progression, indicating a multifaceted role of immune regulators. Population-based longitudinal analyses focusing on neuroimaging (eg, memory task-based functional MRI), biomarker indicators, and AD Braak stage progression in risk allele carriers might provide more support and benefit clinical research and applications. The biological implication of CFH in AD needs further characterization.

FUNDING AND DISCLOSURE

This work was supported by the Strategic Priority Research Program (B) of the Chinese Academy of Sciences (XDB02020003) and Sichuan Province (2014JZ0004). The authors declare no conflict of interest.

ACKNOWLEDGMENTS

We thank Ian Logan for language editing and helpful comments and the three anonymous reviewers for their critical comments on the early version of the manuscript.

REFERENCES

Abecasis GR, Auton A, Brooks LD, DePristo MA, Durbin RM, Handsaker RE *et al* (2012). An integrated map of genetic variation from 1,092 human genomes. *Nature* **491**: 56–65.

Alzheimer's Association (2013). 2013 Alzheimer's disease facts and figures. *Alzheimers Dement* **9**: 208–245.

Ansari M, McKeigue PM, Skerka C, Hayward C, Rudan I, Vitart V *et al* (2013). Genetic influences on plasma CFH and CFHR1 concentrations and their role in susceptibility to age-related macular degeneration. *Hum Mol Genet* **22**: 4857–4869.

Baker ML, Wang JJ, Rogers S, Klein R, Kuller LH, Larsen EK *et al* (2009). Early age-related macular degeneration, cognitive function, and dementia: the Cardiovascular Health Study. *Arch Ophthalmol* **127**: 667–673.

Bergamaschini L, Rossi E, Vergani C, De Simoni MG (2009). Alzheimer's disease: another target for heparin therapy. *Sci World J* **9**: 891–908.

Bertram L, McQueen MB, Mullin K, Blacker D, Tanzi RE (2007). Systematic meta-analyses of Alzheimer disease genetic association studies: the AlzGene database. *Nat Genet* **39**: 17–23.

Bi R, Zhang W, Yu D, Li X, Wang HZ, Hu QX *et al* (2015). Mitochondrial DNA haplogroup B5 confers genetic susceptibility to Alzheimer's disease in Han Chinese. *Neurobiol Aging* **36**: 1604.e7

Bi R, Zhao L, Zhang C, Lu W, Feng JQ, Wang Y *et al* (2014). No association of the LRRK2 genetic variants with Alzheimer's disease in Han Chinese individuals. *Neurobiol Aging* **35**: 444.e5

Blalock EM, Geddes JW, Chen KC, Porter NM, Markesbery WR, Landfield PW (2004). Incipient Alzheimer's disease: microarray correlation analyses reveal major transcriptional and tumor suppressor responses. *Proc Natl Acad Sci USA* **101**: 2173–2178.

Clark SJ, Perveen R, Hakobyan S, Morgan BP, Sim RB, Bishop PN *et al* (2010). Impaired binding of the age-related macular degeneration-associated complement factor H 402H allotype to Bruch's membrane in human retina. *J Biol Chem* **285**: 30192–30202.

Colantuoni C, Lipska BK, Ye T, Hyde TM, Tao R, Leek JT *et al* (2011). Temporal dynamics and genetic control of transcription in the human prefrontal cortex. *Nature* **478**: 519–523.

Crehan H, Hardy J, Pocock J (2012). Microglia, Alzheimer's disease, and complement. *Int J Alzheimers Dis* **2012**: 983640.

DiBattista AM, Stevens BW, Rebeck GW, Green AE (2014). Two Alzheimer's disease risk genes increase entorhinal cortex volume in young adults. *Front Hum Neurosci* **8**: 779.

Donix M, Burggren AC, Scharf M, Marschner K, Suthana NA, Siddarth P *et al* (2013). APOE associated hemispheric asymmetry of entorhinal cortical thickness in aging and Alzheimer's disease. *Psychiatry Res* **214**: 212–220.

Dunckley T, Beach TG, Ramsey KE, Grover A, Mastroeni D, Walker DG *et al* (2006). Gene expression correlates of neurofibrillary tangles in Alzheimer's disease. *Neurobiol Aging* **27**: 1359–1371.

Ferreira VP, Pangburn MK, Cortes C (2010). Complement control protein factor H: the good, the bad, and the inadequate. *Mol Immunol* **47**: 2187–2197.

Filippini N, MacIntosh BJ, Hough MG, Goodwin GM, Frisoni GB, Smith SM *et al* (2009). Distinct patterns of brain activity in young carriers of the APOE-epsilon4 allele. *Proc Natl Acad Sci U S A* **106**: 7209–7214.

Gezen-Ak D, Dursun E, Hanagasi H, Bilgic B, Lohman E, Araz OS *et al* (2013). BDNF, TNFalpha, HSP90, CFH, and IL-10 serum levels in patients with early or late onset Alzheimer's disease or mild cognitive impairment. *J Alzheimers Dis* **37**: 185–195.

Gogtay N, Giedd JN, Lusk L, Hayashi KM, Greenstein D, Vaituzis AC *et al* (2004). Dynamic mapping of human cortical development during childhood through early adulthood. *Proc Natl Acad Sci USA* **101**: 8174–8179.

Hamilton G, Proitsi P, Williams J, O'Donovan M, Owen M, Powell J *et al* (2007). Complement factor H Y402H polymorphism is not associated with late-onset Alzheimer's disease. *Neuromolecular Med* **9**: 331–334.

Harris JA, Devidze N, Verret L, Ho K, Halabisky B, Thwin MT *et al* (2010). Transsynaptic progression of amyloid-beta-induced neuronal dysfunction within the entorhinal-hippocampal network. *Neuron* **68**: 428–441.

Higgins JP, Thompson SG (2002). Quantifying heterogeneity in a meta-analysis. *Stat Med* **21**: 1539–1558.

Honda S, Itoh F, Yoshimoto M, Ohno S, Hinoda Y, Imai K (2000). Association between complement regulatory protein factor H and AM34 antigen, detected in senile plaques. *J Gerontol A Biol Sci Med Sci* **55**: M265–M269.

Hye A, Lynham S, Thambisetty M, Causevic M, Campbell J, Byers HL *et al* (2006). Proteome-based plasma biomarkers for Alzheimer's disease. *Brain* **129**: 3042–3050.

Hye A, Riddoch-Contreras J, Baird AL, Ashton NJ, Bazenet C, Leung R *et al* (2014). Plasma proteins predict conversion to dementia from prodromal disease. *Alzheimers Dement* **10**: 799–807, e792.

Kaarniranta K, Salminen A, Haapasalo A, Soininen H, Hiltunen M (2011). Age-related macular degeneration (AMD): Alzheimer's disease in the eye? *J Alzheimers Dis* **24**: 615–631.

Kadish I, Thibault O, Blalock EM, Chen KC, Gant JC, Porter NM *et al* (2009). Hippocampal and cognitive aging across the lifespan: a bioenergetic shift precedes and increased cholesterol trafficking parallels memory impairment. *J Neurosci* **29**: 1805–1816.

Kamer AR (2010). Systemic inflammation and disease progression in Alzheimer disease. *Neurology* **74**: 1157.

Karch CM, Goate AM (2015). Alzheimer's disease risk genes and mechanisms of disease pathogenesis. *Biol Psychiatry* **77**: 43–51.

Keenan TD, Goldacre R, Goldacre MJ (2014). Associations between age-related macular degeneration, Alzheimer disease, and dementia: record linkage study of hospital admissions. *JAMA Ophthalmol* **132**: 63–68.

Khan UA, Liu L, Provenzano FA, Berman DE, Profaci CP, Sloan R *et al* (2014). Molecular drivers and cortical spread of lateral entorhinal cortex dysfunction in preclinical Alzheimer's disease. *Nat Neurosci* **17**: 304–311.

Klein RJ, Zeiss C, Chew EY, Tsai JY, Sackler RS, Haynes C *et al* (2005). Complement factor H polymorphism in age-related macular degeneration. *Science* **308**: 385–389.

Lambert JC, Ibrahim-Verbaas CA, Harold D, Naj AC, Sims R, Bellenguez C *et al* (2013). Meta-analysis of 74,046 individuals identifies 11 new susceptibility loci for Alzheimer's disease. *Nat Genet* **45**: 1452–1458.

Le Fur I, Laumet G, Richard F, Fievet N, Berr C, Rouaud O *et al* (2010). Association study of the CFH Y402H polymorphism with Alzheimer's disease. *Neurobiol Aging* **31**: 165–166.

Li J, Cui Y, Wu K, Liu B, Zhang Y, Wang C *et al* (2015). The cortical surface area of the insula mediates the effect of DBH rs7040170 on novelty seeking. *Neuroimage* **117**: 184–190.

Lu T, Pan Y, Kao SY, Li C, Kohane I, Chan J *et al* (2004). Gene regulation and DNA damage in the ageing human brain. *Nature* **429**: 883–891.

O'Dwyer L, Lamberton F, Matura S, Tanner C, Scheibe M, Miller J *et al* (2012). Reduced hippocampal volume in healthy young ApoE4 carriers: an MRI study. *PLoS One* **7**: e48895.

Ormsby RJ, Ranganathan S, Tong JC, Griggs KM, Dimasi DP, Hewitt AW *et al* (2008). Functional and structural implications of the complement factor H Y402H polymorphism associated with age-related macular degeneration. *Invest Ophthalmol Vis Sci* **49**: 1763–1770.

Patel D, Henry J, Good T (2006). Attenuation of beta-amyloid induced toxicity by sialic acid-conjugated dendrimeric polymers. *Biochim Biophys Acta* **1760**: 1802–1809.

Pham TQ, Kifley A, Mitchell P, Wang JJ (2006). Relation of age-related macular degeneration and cognitive impairment in an older population. *Gerontology* **52**: 353–358.

Proitsi P, Lupton MK, Dudbridge F, Tsolaki M, Hamilton G, Daniilidou M *et al* (2012). Alzheimer's disease and age-related macular degeneration have different genetic models for complement gene variation. *Neurobiol Aging* **33**: 1843.e9

Purcell S, Neale B, Todd-Brown K, Thomas L, Ferreira MA, Bender D *et al* (2007). PLINK: a tool set for whole-genome association and population-based linkage analyses. *Am J Hum Genet* **81**: 559–575.

Querfurth HW, LaFerla FM (2010). Alzheimer's disease. *N Engl J Med* **362**: 329–344.

Ramasamy A, Trabzuni D, Guelfi S, Varghese V, Smith C, Walker R *et al* (2014). Genetic variability in the regulation of gene expression in ten regions of the human brain. *Nat Neurosci* **17**: 1418–1428.

Ritchie MD, Hahn LW, Roodi N, Bailey LR, Dupont WD, Parl FF *et al* (2001). Multifactor-dimensionality reduction reveals high-order interactions among estrogen-metabolism genes in sporadic breast cancer. *Am J Hum Genet* **69**: 138–147.

Shaw P, Lerch JP, Pruessner JC, Taylor KN, Rose AB, Greenstein D *et al* (2007). Cortical morphology in children and adolescents with different apolipoprotein E gene polymorphisms: an observational study. *Lancet Neurol* **6**: 494–500.

Sivak JM (2013). The aging eye: common degenerative mechanisms between the Alzheimer's brain and retinal disease. *Invest Ophthalmol Vis Sci* **54**: 871–880.

Strang F, Scheichl A, Chen YC, Wang X, Htun NM, Bassler N *et al* (2012). Amyloid plaques dissociate pentameric to monomeric C-reactive protein: a novel pathomechanism driving cortical inflammation in Alzheimer's disease? *Brain Pathol* **22**: 337–346.

Strohmeyer R, Ramirez M, Cole GJ, Mueller K, Rogers J (2002). Association of factor H of the alternative pathway of complement with agrin and complement receptor 3 in the Alzheimer's disease brain. *J Neuroimmunol* **131**: 135–146.

Strohmeyer R, Shen Y, Rogers J (2000). Detection of complement alternative pathway mRNA and proteins in the Alzheimer's disease brain. *Brain Res Mol Brain Res* **81**: 7–18.

Suh SW, Jensen KB, Jensen MS, Silva DS, Kesslak PJ, Danscher G *et al* (2000). Histochemically-reactive zinc in amyloid plaques, angiopathy, and degenerating neurons of Alzheimer's diseased brains. *Brain Res* **852**: 274–278.

Thambisetty M, Hye A, Foy C, Daly E, Glover A, Cooper A *et al* (2008). Proteome-based identification of plasma proteins associated with hippocampal metabolism in early Alzheimer's disease. *J Neurol* **255**: 1712–1720.

The GTEx Consortium (2013). The Genotype-Tissue Expression (GTEx) project. *Nat Genet* **45**: 580–585.

Voight BF, Kudaravalli S, Wen X, Pritchard JK (2006). A map of recent positive selection in the human genome. *PLoS Biol* **4**: e72.

Voineskos AN, Lerch JP, Felsky D, Shaikh S, Rajji TK, Miranda D *et al* (2011). The brain-derived neurotrophic factor Val66Met polymorphism and prediction of neural risk for Alzheimer disease. *Arch Gen Psychiatry* **68**: 198–206.

Wang HZ, Bi R, Hu QX, Xiang Q, Zhang C, Zhang DF *et al* (2014). Validating GWAS-identified risk loci for Alzheimer's disease in Han Chinese populations. *Mol Neurobiol*. (doi:10.1007/s12035-014-9015-z).

Weiner MW, Aisen PS, Jack CR Jr, Jagust WJ, Trojanowski JQ, Shaw L *et al* (2010). The Alzheimer's disease neuroimaging initiative: progress report and future plans. *Alzheimers Dement* **6**: 202–211 e207.

Wong WL, Su X, Li X, Cheung CM, Klein R, Cheng CY *et al* (2014). Global prevalence of age-related macular degeneration and disease burden projection for 2020 and 2040: a systematic review and meta-analysis. *Lancet Glob Health* **2**: e106–e116.

Woo SJ, Park KH, Ahn J, Choe JY, Jeong H, Han JW *et al* (2012). Cognitive impairment in age-related macular degeneration and geographic atrophy. *Ophthalmology* **119**: 2094–2101.

Wyss-Coray T (2006). Inflammation in Alzheimer disease: driving force, bystander or beneficial response? *Nat Med* **12**: 1005–1015.

Zetterberg M, Landgren S, Andπersson ME, Palmer MS, Gustafson DR, Skoog I *et al* (2008). Association of complement factor H Y402H gene polymorphism with Alzheimer's disease. *Am J Med Genet B Neuropsychiatr Genet* **147B**: 720–726.

Zhang DF, Wang D, Li YY, Yao YG (2014). Mapping genetic variants in the CFH gene for association with leprosy in Han Chinese. *Genes Immun* **15**: 506–510.

Zhang J (2003). Evolution of the human ASPM gene, a major determinant of brain size. *Genetics* **165**: 2063–2070.

Zhang X, Yu JT, Li J, Wang C, Tan L, Liu B *et al* (2015). Bridging Integrator 1 (BIN1) genotype effects on working memory, hippocampal volume, and functional connectivity in young healthy individuals. *Neuropsychopharmacology* **40**: 1794–1803.

Supplementary Information accompanies the paper on the Neuropsychopharmacology website (http://www.nature.com/npp)

Supplemental Methods

SNP selection, genotyping, and association analysis

The 17 SNPs of five immune genes (*CR1*, *CR2*, *CLU*, *CD33*, *TREML2*) that were identified as the top Alzheimer's susceptibility genes in Europeans (Bertram *et al*, 2007; Lambert *et al*, 2013), are composed of genome-wide association study (GWAS) top hits, tagging SNPs and potentially functional SNPs of the five top genes (Table S1). The 11 *CFH* SNPs, which cover more than 80% of the entire gene (Fig. S1), were selected according to the criteria described in our previous study (Zhang *et al*, 2014). Among these selected SNPs, nine (rs800292, rs10801555, rs10922096, rs10733086, rs10737680, rs11582939, rs2019727, rs1410996 and rs426736) were tag SNPs, three (rs800292, p.V62I; rs1061170, p.Y402H; rs460184, p.V1197A) were functional variants in three important domains of the CFH protein.

All the SNPs were genotyped by using the SNaPshot assay as described in our previous study (Zhang *et al*, 2014). The *APOE* ε4, the major risk factor for AD, was genotyped as previously described (Bi *et al*, 2015; Bi *et al*, 2014; Wang *et al*, 2014) . The genotyping results from the SNaPshot assay were double checked and further confirmed by direct sequencing 2% of the total samples.

Association analysis was carried out using PLINK (Purcell *et al*, 2007). Genotypes were checked for departures from the Hardy-Weinberg equilibrium (HWE) in control populations. Allelic (Table 1) and genotypic (Table S2) comparisons with 2 df genotypic, Cochran-Armitage trend, dominant, and recessive models were conducted for individual SNPs. We pooled all samples from the general populations as a combined sample for Chinese (termed "Combined Chinese") and Europeans (termed "Combined Europeans"), respectively. Comparison of the genotype counts between the combined case and control populations was estimated by the Chi square test. Meta-analysis for the association of *CFH* SNPs with AD in the two combined sample sets was performed by using Review manager (RevMan 5.2, http://tech.cochrane.org/revman), with the Cochran-Mantel-Haenszel method under a fixed effect. The heterogeneity was measured by the I^2 index (Higgins and Thompson, 2002). The genetic associations were explored further by estimating the significance of SNP-SNP interaction using the multifactor-dimensionality reduction (MDR) method (Ritchie *et al*, 2001) or the "--epistasis" command in PLINK (Purcell *et al*, 2007).

Neuroimaging analysis for the effects of *CFH* variants on structural and functional brain changes

We recruited 360 healthy young adults (age 19.4 ± 1.1 years; 51.7% men) to study the effects of the five potential Alzheimer's risk SNPs (rs1061170, rs800292, rs426736, rs1410996, and rs11582939) on morphological changes of the brain. All participants were university students with no history of neuropsychiatric disorders or acquired brain injury. After a full explanation, all participants gave written informed consent.

Magnetic resonance imaging (MRI) scans were performed on a MR750 3.0 Tesla magnetic resonance scanner (GE Healthcare). High-resolution 3D T1-weighted brain

volume (BRAVO) MRI sequence was subsequently performed with the following parameters: TR = 8.16 ms, TE = 3.18 ms, flip angle = 7°, FOV = 256 mm × 256 mm, voxel size = 1 × 1 × 1 mm^3, and 188 slices. MRI data were analyzed with FreeSurfer software (version 5.3) package (http://surfer.nmr.mgh.harvard.edu/). First, we performed a whole-brain Voxel-Based Morphometry (VBM) analysis for volume and density of the gray matter. Second, we detected the effect of the AD-risk *CFH* SNPs on total intracranial volume (ICV) and hippocampus volume changes. Finally, we tested the effect of the AD-risk *CFH* SNPs on the thickness of the entorhinal cortex (Harris *et al*, 2010; Khan *et al*, 2014).

For each subject, the cortical surface was reconstructed using an automated procedure (Dale *et al*, 1999; Fischl *et al*, 1999). Once generated, the cortical surface model was inspected and manually edited for technical accuracy; minimal manual correction was performed on any inaccuracies in Talairach-transformation, skull stripping and segmentation, and the model re-inspected. The reconstructed surface was then divided into distinct cortical regions (Fischl *et al*, 2004), and the average thickness values of the entorhinal cortex in each hemisphere were measured. To test the effect of *CFH* genotypes on the thickness of the entorhinal cortex, we applied a general linear regression model, with *CFH* genotypes as predictors for the thickness of the entorhinal cortex. To control for the confounding effect of gender, age and education year and ICV, a preliminary regression analysis was conducted, with the four factors as independent variables, and the lateral entorhinal cortical thickness or lateral hippocampal volume as a dependent variable, the residual for each subject was used to indicate the hippocampal volume or the entorhinal cortical thickness for use in the later analysis.

As we observed no significant association between ICV and *CFH* risk SNPs and between hippocampus volume change and *CFH* risk SNPs in the pilot statistical analysis, we then only focused on the entorhinal cortical thickness, and ten linear regression analyses (5 SNPs x 2 hemisphere) were conducted separately to test the main effect of each SNP. To correct for multiple comparisons, the statistical significance level was set as $P < 0.005$ (0.05/10[tests], Bonferroni correction). All statistical analyses were carried out in SPSS15.0 for Windows (SPSS, Chicago, IL, USA).

Expression Quantitative Trait Loci (eQTL) analysis

Ten brain regions, cerebellar cortex (CRBL); frontal cortex (FCTX); hippocampus (HIPP); medulla (specifically inferior olivary nucleus, MEDU); occipital cortex (specifically primary visual cortex, OCTX); putamen (PUTM); substantia nigra (SNIG), temporal cortex (TCTX); thalamus (THAL) and intralobular white matter (WHMT) were included in the eQTL analysis. All 134 individuals were confirmed to be neuropathologically normal and European-descent. Details were shown in the brain eQTL database (http://caprica.genetics.kcl.ac.uk/BRAINEAC/) (Ramasamy *et al*, 2014).

Construction of U251 cells with stable expression of the mutant APP (APP^{Mut})

and PSEN1 ($PSEN1^{Mut}$) genes

The CDS region of the *APP* gene and *PSEN1* gene with flag tag were cloned into PLVX vector of the Lenti-X Tet-On Advanced Inducible Expression System (Clontech). Mutations *APP*-p.M671L and *PSEN1*-p.M139V/M146L/H163R were introduced into PLVX-APP and PLVX-PSEN1 vectors, respectively, by using site-directed mutagenesis PCR method.

U251 cells were maintained in RPMI 1640 supplemented with 10% fetal bovine serum (FBS) (Gibco, USA, 11875). HEK293T cells were cultured in DMEM (Gibco, USA, 11965) containing 10% heat inactivated FBS. U251 cells with stable expression of the mutant *APP* (M671L) or *PSEN1* (M139V/M146L/H163R) were constructed according to the instruction of Lenti-X Tet-On Advanced Inducible Expression System (Clontech) and following our previously reported method (Bi *et al*, 2015). In brief, the response lentivirus system was composed of mutant PLVX-APP or PLVX-PSEN1 constructs, packaging plasmid psPAX2 (Addgene, England, 12260) and envelope plasmid PMD2.G (Addgene, England, 12259), while the regulator lentivirus system was composed of PLVX-Tet-On-Advanced vector, psPAX2 and PMD2.G. The lentivirus supernatant was produced from HEK293T cells and was used to infect U251 cells with the ratio of 4:1 for the response lentivirus and the regulator lentivirus. Cells were selected in growth medium with 500 μg/mL G418 and 1μg/mL puromycin.

Determination of *CFH* mRNA level in β-amyloid 1-42 ($A\beta_{1-42}$) treated U251 cells or in cells with overexpression of APP^{Mut} or $PSEN1^{Mut}$

Control U251 cells, U251 cells with PLVX vector (PLVX), U251 cells with APP^{Mut}, and U251 cells with $PSEN1^{Mut}$ were cultured in 12-well plate with 1 μg/mL doxycycline (Sigma) for 24 hours to induce the expression of APP^{Mut} and $PSEN1^{Mut}$.

Control U251 cells were cultured in 12-well plate and were treated with 20 μM of $A\beta_{1-42}$ for 24 hours. Total RNA was extracted using TRIZOL (Invitrogen, Carlsbad, CA). cDNA was synthesized with 1 μg of total RNA and M-MLV Reverse Transcriptase (Promega) in a total volume of 25 μL reaction mixture according to the manufacturer's instructions.

Quantitative real-time PCR was used to determine the relative mRNA level of the *CFH* gene following the approach described in our previous study (Feng *et al*, 2013). In brief, *CFH* mRNA level was measured by primer pair (CFH-RT-U1: 5'-GCTGGTCTCCTACTCCCAGA-3'; CFH-RT-L: 5'-TTCGCTTTTTCTTTTAAGGCA-3') and was normalized to the housekeeping gene GAPDH (GAPDH-RT-F: 5'-CAACTACATGGTTTACATGTTC-3'; GAPDH-RT-F: 5'-GCCAGTGGACTCCACGAC-3'). Quantitative real-time PCR were performed on the MyiQ2 system (BioRad Laboratories, Hercules, CA, USA) with the SYBR Premix ExTaq II (TaKaRa).

Western blot

Total cell protein was obtained by using cell lysis buffer (Beyotime, China, P0013) and the protein concentration was determined by BCA Protein Assay Kit (Beyotime,

China, P0012). Cell supernatant was collected for determination of Aβ. A total of 20 μg protein or 16 μL of cell supernatant was separated in 12% SDS polyacrylamide gel electrophoresis (PAGE) and transferred to a polyvinylidene difluoride membrane (Bio-Rad, USA, 162-0177). The primary antibody include: monoclonal mouse antibodies against flag tag (Abmart, China, M20008) (1:5000, overnight at 4 °C) or Actin (EnoGene, China, E12-042; as protein loading control) (1:2000, overnight at 4 °C), monoclonal rabbit antibodies against APP (Cell Signaling, #2450) (1:1000, overnight at 4 °C) or Aβ (Cell Signaling, #8243) (1:1000, overnight at 4 °C). The secondary antibody was anti-mouse or anti-rabbit IgG peroxidase-conjugated secondary antibody (KPL) (1:10000, 1 hour at room temperature). Immobilon Western Chemiluminescent HRP Substrate (Millipore, USA, WBKLS0500) was used to visualize the epitope.

Supplemental Results

Table S1. Screening for association of AD related top immune genes (as identified in Europeans) in Han Chinese with AD

Gene	SNP	MAF (case/control)	*P*-value	OR (95%CI)	Annotation
CR1	rs6656401	0.039/0.026	0.184	1.516 (0.817-2.811)	tag
	rs10127904	0.061/0.035	0.022	1.830 (1.085-3.086)	tag
	rs6691117	0.229/0.209	0.381	1.125 (0.865-1.464)	I2065V
	rs3818361	0.364/0.359	0.870	1.019 (0.812-1.278)	tag
	rs12034383	0.444/0.449	0.850	0.979 (0.786-1.219)	tag
	rs1408077	0.365/0.361	0.861	1.020 (0.814-1.280)	tag
	rs10779339	0.341/0.362	0.438	0.914 (0.727-1.148)	3'UTR
CR2	rs17615	0.109/0.108	0.932	1.015 (0.715-1.441)	S639N
	rs17045328	0.312/0.326	0.598	0.939 (0.743-1.186)	tag
	rs9429940	0.039/0.043	0.747	0.913 (0.526-1.584)	3'UTR
CLU	rs11136000	0.210/0.185	0.200	1.170 (0.920-1.487)	GWAS
	rs9331942	0.325/0.356	0.178	0.871 (0.711-1.065)	tag
CD33	rs3865444	0.208/0.201	0.731	1.042 (0.823-1.321)	GWAS
TREML2	rs2093395	0.367/0.356	0.6399	1.050 (0.856-1.287)	eQTL
	rs3747742	0.367/0.358	0.7128	1.039 (0.848-1.274)	eQTL
	rs11752528	0.105/0.101	0.7803	1.047 (0.758-1.447)	eQTL
	rs1484268	0.449/0.440	0.7288	1.036 (0.850-1.261)	eQTL

Note: Genotyping of these SNPs was performed in our Stage 1 samples including 380 AD patients and 475 healthy individuals from East China. GWAS top hits, tagging and functional SNPs were genotyped (refer to the main text for more information). Shown *P* values are allelic association *P*-values.

MAF – minor allele frequency.

Table S2. Genotypic associations of *CFH* variants with AD in Chinese populations

SNP	Allele	TEST	Stage1 (SH: AD1 vs PC1)			Stage2-1 (SC: AD2 vs PC2)			Stage 2-2 (SC: AD2 vs LC)			Combined (AD1+AD2 vs PC1+PC2)		
			AFF	UNAFF	*P*	AFF	UNAFF	*P*	AFF	UNAFF	*P*	AFF	UNAFF	*P*
rs800292	T/C	GENO	45/183/149	75/232/168	0.203	32/193/117	62/173/102	0.003	32/193/117	82/263/156	0.014	77/376/266	137/405/270	0.002
		TREND	273/481	382/568	0.087	257/427	297/377	0.010	257/427	427/575	0.027	530/908	679/945	0.004
		DOM	228/149	307/168	0.213	225/117	235/102	0.272	225/117	345/156	0.349	453/266	542/270	0.125
		REC	45/332	75/400	0.108	32/310	62/275	0.001	32/310	82/419	0.003	77/642	137/675	0.001
rs1061170	C/T	GENO	1/48/328	0/37/437	0.030	4/41/291	1/27/309	0.074	4/41/291	4/29/467	0.004	5/89/619	1/64/746	0.002
		TREND	50/704	37/911	0.010	49/623	29/645	0.024	49/623	37/963	0.002	99/1327	66/1556	0.001
		DOM	49/328	37/437	0.013	45/291	28/309	0.034	45/291	33/467	0.001	94/619	65/746	0.001
		REC	1/376	0/474	0.262	4/332	1/336	0.177	4/332	4/496	0.570	5/708	1/810	0.072
rs10801555	A/G	GENO	1/31/345	0/38/437	0.528	2/35/305	1/27/309	0.508	2/35/305	4/44/453	0.733	3/66/650	1/65/746	0.374
		TREND	33/721	38/912	0.697	39/645	29/645	0.247	39/645	52/950	0.661	72/1366	67/1557	0.245
		DOM	32/345	38/437	0.797	37/305	28/309	0.266	37/305	48/453	0.558	69/650	66/746	0.312
		REC	1/376	0/475	0.261	2/340	1/336	0.572	2/340	4/497	0.717	3/716	1/811	0.261
rs10922096	T/C	GENO	7/78/292	4/114/357	0.241	5/64/271	5/64/268	0.998	5/64/271	12/91/398	0.636	12/142/563	9/178/625	0.403
		TREND	92/662	122/828	0.688	74/606	74/600	0.955	74/606	115/887	0.715	166/1268	196/1428	0.673
		DOM	85/292	118/357	0.435	69/271	69/268	0.954	69/271	103/398	0.926	154/563	187/625	0.467
		REC	7/370	4/471	0.193	5/335	5/332	0.989	5/335	12/489	0.350	12/705	9/803	0.343
rs2019727	T/A	GENO	2/51/324	3/81/391	0.359	2/31/309	1/46/290	0.148	2/31/309	7/46/448	0.528	4/82/633	4/127/681	0.055
		TREND	55/699	87/863	0.164	35/649	48/626	0.125	35/649	60/942	0.476	90/1348	135/1489	0.029
		DOM	53/324	84/391	0.152	33/309	47/290	0.082	33/309	53/448	0.661	86/633	131/681	0.020
		REC	2/375	3/472	0.848	2/340	1/336	0.572	2/340	7/494	0.260	4/715	4/808	0.863
rs10733086	A/T	GENO	1/41/335	0/57/418	0.470	2/43/296	2/39/296	0.918	2/43/296	5/60/436	0.786	3/84/631	2/96/714	0.840

		TREND	43/711	57/893	0.791	47/635	43/631	0.708	47/635	70/932	0.942	90/1346	100/1524	0.900
		DOM	42/335	57/418	0.697	45/296	41/296	0.687	45/296	65/436	0.925	87/631	98/714	0.977
		REC	1/376	0/475	0.261	2/339	2/335	0.991	2/339	5/496	0.519	3/715	2/810	0.557
rs10737680	C/A	GENO	52/194/131	85/238/152	0.253	52/205/85	66/161/110	0.006	52/205/85	82/270/149	0.198	104/399/216	151/399/262	0.024
		TREND	298/456	408/542	0.145	309/375	293/381	0.507	309/375	434/568	0.414	607/831	701/923	0.582
		DOM	246/131	323/152	0.398	257/85	227/110	0.025	257/85	352/149	0.120	503/216	550/262	0.349
		REC	52/325	85/390	0.106	52/290	66/271	0.132	52/290	82/419	0.650	104/615	151/661	0.030
rs1410996	T/C	GENO	51/193/133	85/237/153	0.205	40/215/87	64/164/109	0.001	40/215/87	83/268/150	0.019	91/408/220	149/401/262	0.002
		TREND	295/459	407/543	0.114	295/389	292/382	0.938	295/389	434/568	0.934	590/848	699/925	0.240
		DOM	244/133	322/153	0.346	255/87	228/109	0.047	255/87	351/150	0.153	499/220	550/262	0.483
		REC	51/326	85/390	0.084	40/302	64/273	0.008	40/302	83/418	0.049	91/628	149/663	0.002
rs11582939	T/C	GENO	68/198/111	108/253/114	0.099	54/207/81	87/170/80	0.003	54/207/81	114/269/118	0.036	149/405/165	188/423/201	0.246
		TREND	334/420	469/481	0.031	315/369	344/330	0.051	315/369	497/505	0.125	703/735	799/825	0.857
		DOM	266/111	361/114	0.073	261/81	257/80	0.987	261/81	383/118	0.965	554/165	611/201	0.409
		REC	68/309	108/367	0.092	54/288	87/250	0.001	54/288	114/387	0.013	149/570	188/624	0.252
rs426736	C/T	GENO	111/179/87	109/217/149	0.012	64/210/68	89/161/87	0.002	64/210/68	110/270/121	0.095	179/389/151	196/378/238	0.001
		TREND	401/353	435/515	0.003	338/346	339/335	0.733	338/346	490/512	0.824	747/691	770/854	0.012
		DOM	290/87	326/149	0.007	274/68	250/87	0.066	274/68	380/121	0.145	568/151	574/238	0.0002
		REC	111/266	109/366	0.031	64/278	89/248	0.016	64/278	110/391	0.253	179/540	196/616	0.731

Note: AD1, patients with AD of stage 1 from Shanghai (SH); PC1, population controls of stage 1 from Shanghai; AD2, patients with AD of stage 2 from Sichuan (SC); PC2, population controls of stage 2 from Sichuan; LC, longevity controls of stage 2 from Sichuan; AFF, genotype counts in cases; UNAFF, genotype counts in controls; *P*, association *p*-values given by PLINK using the --model option; GENO, genotypic (2 df) test; TREND, Cochran-Armitage trend test; DOM, dominant gene action (1df) test; REC, recessive gene action (1df) test.

Table S3. Association results of 5 *CFH* SNPs with bilateral hippocampal volume in 360 healthy young adults

SNP	Left hippocampal volume		Right hippocampal volume	
	F (1, 358)	*P*	F (1, 358)	*P*
rs1061170	0.022	0.883	1.002	0.318
rs800292	0.153	0.696	0.122	0.727
rs426736	0.812	0.368	0.001	0.973
rs1410996	0.082	0.775	0.064	0.801
rs11582939	0.257	0.613	0.321	0.571

Note: *P* – linear regression *P*-value

Table S4. Results of 5 *CFH* SNPs and their effects on bilateral entorhinal cortical thickness in 360 healthy young adults

SNP	Encode	Genotype	Counts	Frequency	Left entorhinal cortex			Right entorhinal cortex		
					Cortical thickness	F	*P*	Cortical thickness	F	*P*
rs1061170	1[a]	CC+CT	36	0.10	3.3541±0.27455	5.128	0.024	3.6041±0.36436	9.287	**2.5x10^{-3}**
	2	TT	324	0.90	3.2326±0.31418			3.4099±0.37053		
rs800292[a]	1	CC	124	0.34	3.2931±0.32068	3.436	0.065	3.5039±0.35509	12.454	**4.7x10^{-4}**
	2	CT	176	0.49	3.2205±0.32140			3.4192±0.36334		
	3	TT	60	0.17	3.2161±0.25480			3.3049±0.41102		
rs426736	1	CC	97	0.27	3.2981±0.31290	0.979	0.323	3.4804±0.36139	3.388	0.066
	2	CT	177	0.49	3.2110±0.33255			3.4244±0.35471		
	3	TT	86	0.24	3.2540±0.25786			3.3820±0.42125		
rs1410996	1	CC	127	0.35	3.2888±0.31340	1.542	0.215	3.4899±0.34008	6.645	0.010
	2	CT	168	0.47	3.2102±0.32471			3.4115±0.37465		
	3	TT	65	0.18	3.2481±0.26720			3.3571±0.42098		
rs11582939	1	CC	85	0.24	3.2526±0.25908	0.191	0.662	3.3774±0.42162	3.232	0.073
	2	CT	172	0.48	3.2246±0.33285			3.4289±0.35994		
	3	TT	103	0.28	3.2718±0.31726			3.4729±0.35292		

Note: The effects of 5 AD risk SNPs (rs1061170, rs800292, rs426736, rs1410996, and rs11582939) on brain structural changes (here thickness of bilateral entorhinal cortex) were measured in 360 healthy young adults (age: 19.4 ± 1.1 years old; male: 51.7%) by Magnetic resonance imaging (MRI) scans. Linear regression analyses were conducted to test the main effect of each SNP. *P* values less than 0.005 (0.05/10[tests]) were marked in bold.

Table S5. Association of rs800292 with mild cognitive impairment (MCI) in the ADNI_1 cohort

SNP	A1	A2	TEST	AFF	UNAFF	*P-value*
rs800292	T	C	GENO	17/131/215	25/80/109	0.004581
rs800292	T	C	TREND	165/561	130/298	0.004776
rs800292	T	C	ALLELIC	165/561	130/298	0.004022
rs800292	T	C	DOM	148/215	105/109	0.05244
rs800292	T	C	REC	17/346	25/189	0.001772

Note: A1, effect allele (minor allele); A2, reference allele (major allele); AFF, genotype counts in the cases (MCI); UNAFF, genotype counts in controls; GENO, genotypic (2 df) test; TREND, Cochran-Armitage trend test; DOM, dominant gene action (1df) test; REC, recessive gene action (1df) test; *P-value*, association *p*-values given by the PLINK using the --model option.

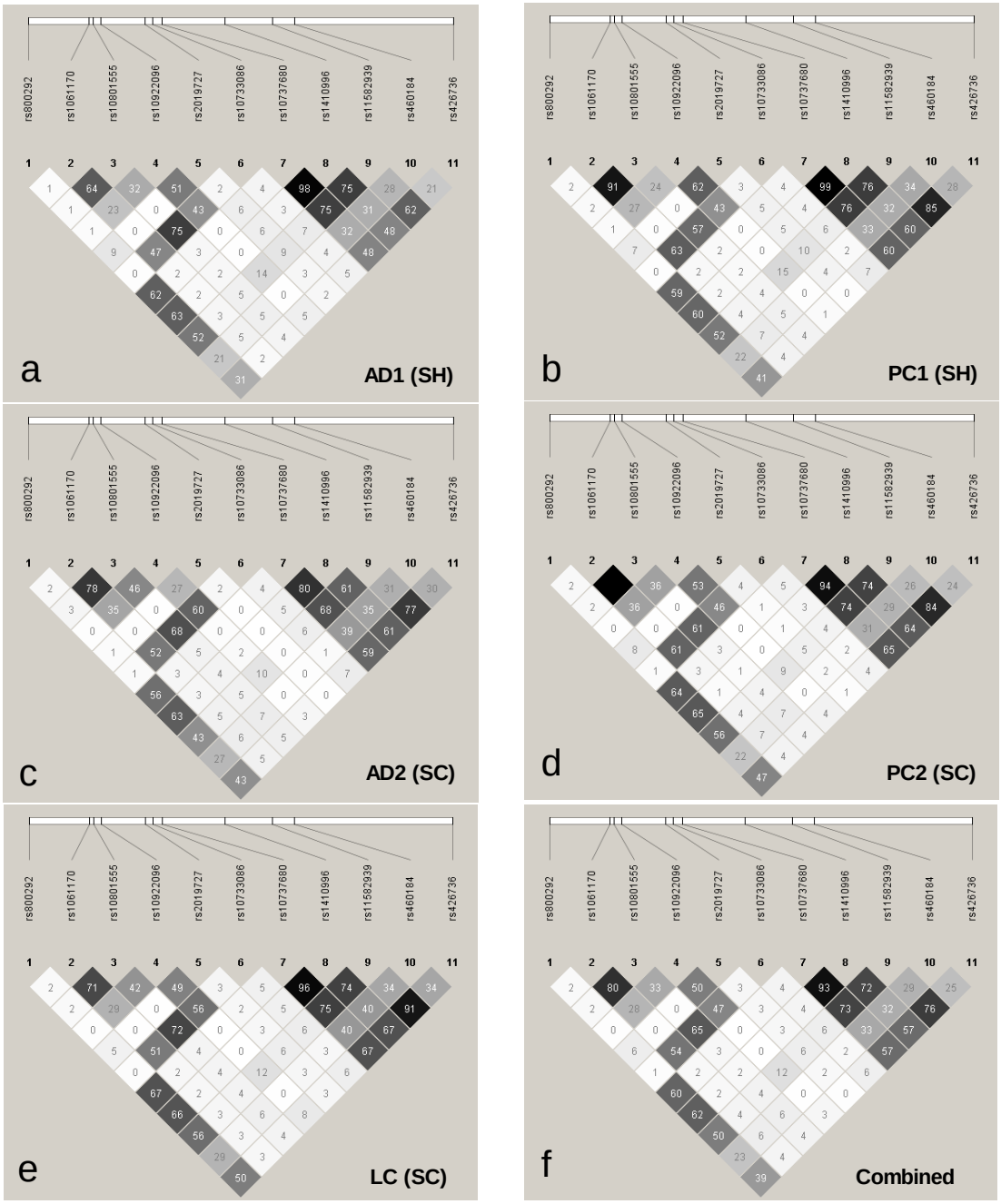

Figure S1. Linkage disequilibrium (LD) pattern of the 11 analyzed *CFH* SNPs in all our populations. Results were performed by Haploview 4.2 based on the data obtained in this study. r^2 was used for the LD color scheme. Black squares represent high LD as measured by r^2, gradually coloring down to white squares of low LD. The individual square showed the 100 ×r^2 value for each SNP pair. **(a)** AD1, patients with AD from East China (SH); **(b)** PC1, healthy individuals from the matched general population; **(c)** AD2, patients with AD from Sichuan (SC), Southwest China; **(d)** PC2, healthy population controls from Sichuan, Southwest China; **(e)** LC, healthy longevity subjects from Sichuan, Southwest China. **(f)** Combined samples including AD1, PC1, AD2, and PC2.

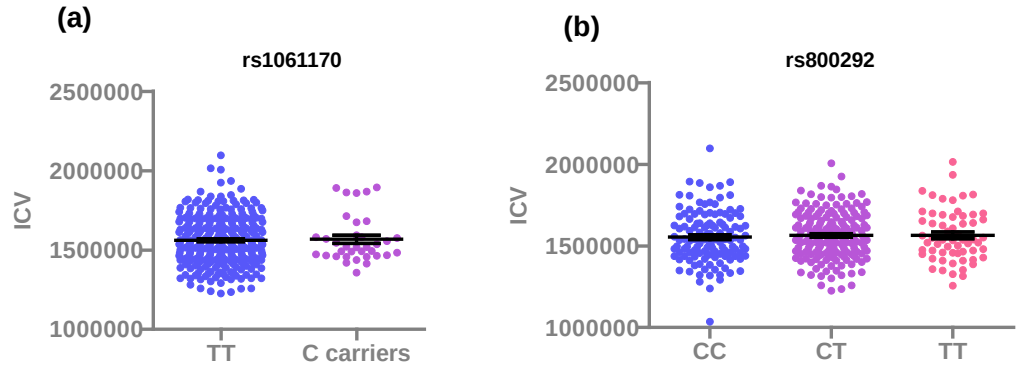

Figure S2. Effect of *CFH* genotypes on estimated total intracranial volume (ICV). Only the two most significant AD risk SNPs (rs1061170 and rs800292) were analyzed. Linear regression analyses were conducted to test the main effect of each SNP. No significant effects were observed.

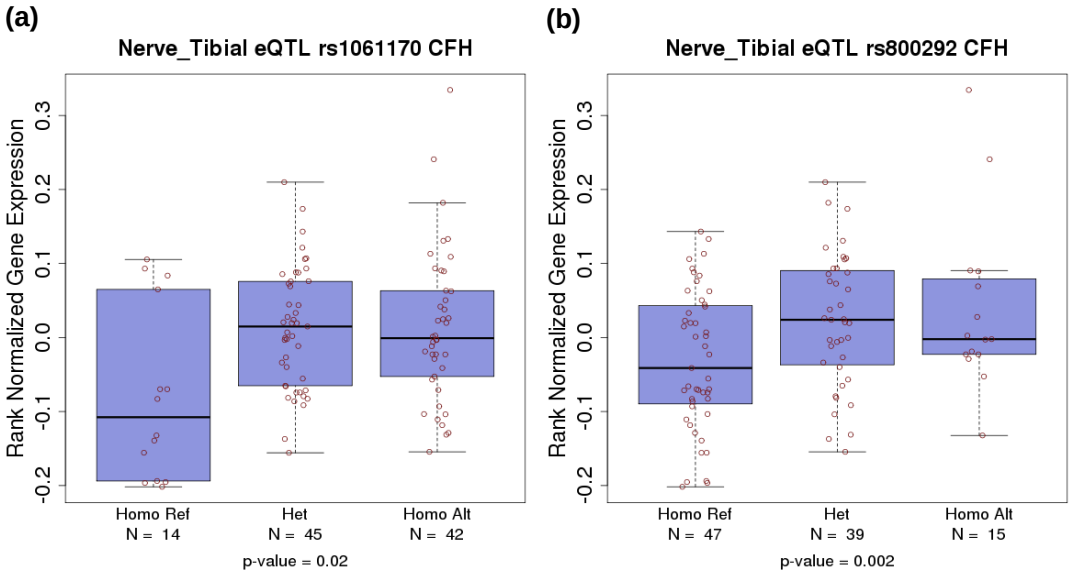

Figure S3. Effect of rs1061170 and rs800292 genotypes on *CFH* mRNA expression changes in tibial nerves. GTEx, the Genotype-Tissue Expression project (http://www.gtexportal.org/home/), provides a comprehensive atlas of gene expression and regulation across multiple human tissues (The GTEx Consortium, 2013).

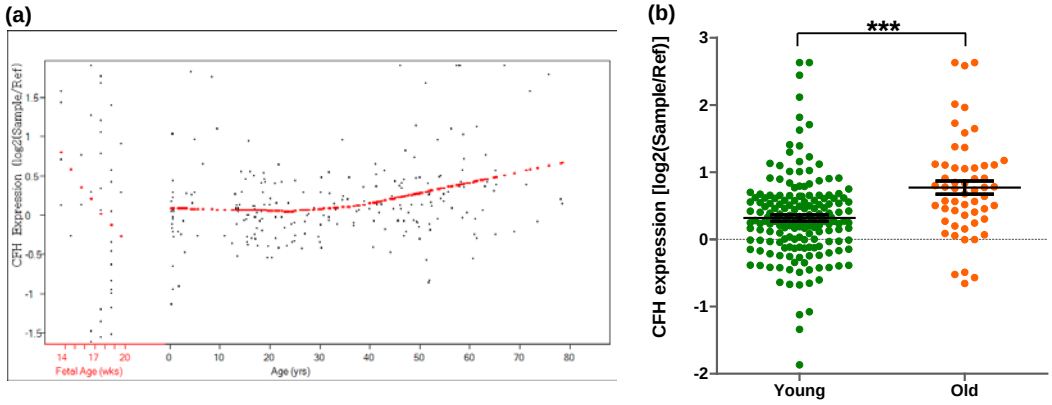

Figure S4. Expression pattern of the *CFH* gene in human postmortem prefrontal cortex across the lifespan. Expression data of 272 human postmortem dorsolateral prefrontal cortex of normal subjects across the lifespan was retrieved from BrainCloud (cf. http://braincloud.jhmi.edu/) (Colantuoni *et al*, 2011). (a) *CFH* expression pattern in prefrontal cortex across the lifespan. (b) *CFH* expression changes with aging in postnatal individuals. Young, postnatal individuals less than 50 years old; Old, postnatal individuals more than 50 (include) years old; *Student's t* test was performed to evaluate the expression difference between the two groups. Data represent mean ± SEM. **** $P < 0.001$

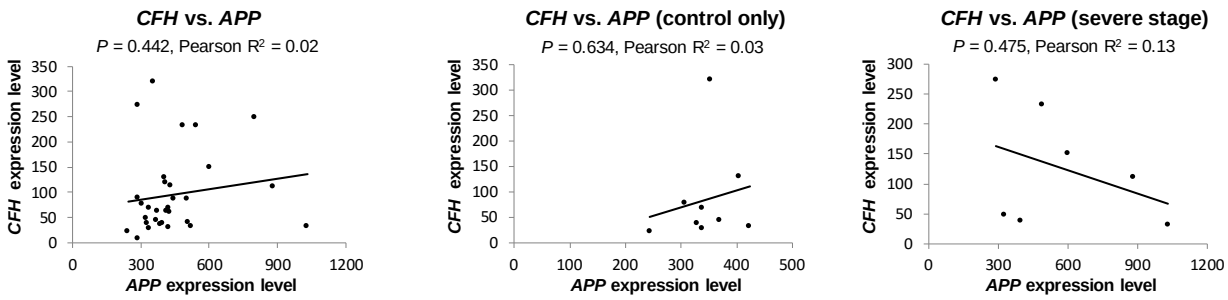

Figure S5. Correlation between *CFH* mRNA level and *APP* mRNA level in hippocampus of AD patients or controls. *CFH* (213800_at) and *APP* (probe 211277_x_at) expression data in hippocampal samples from 22 postmortems showing AD at different stages of severity was retrieved from GEO (http://www.ncbi.nlm.nih.gov/sites/GDSbrowser, GSE1297) (Blalock *et al*, 2004).

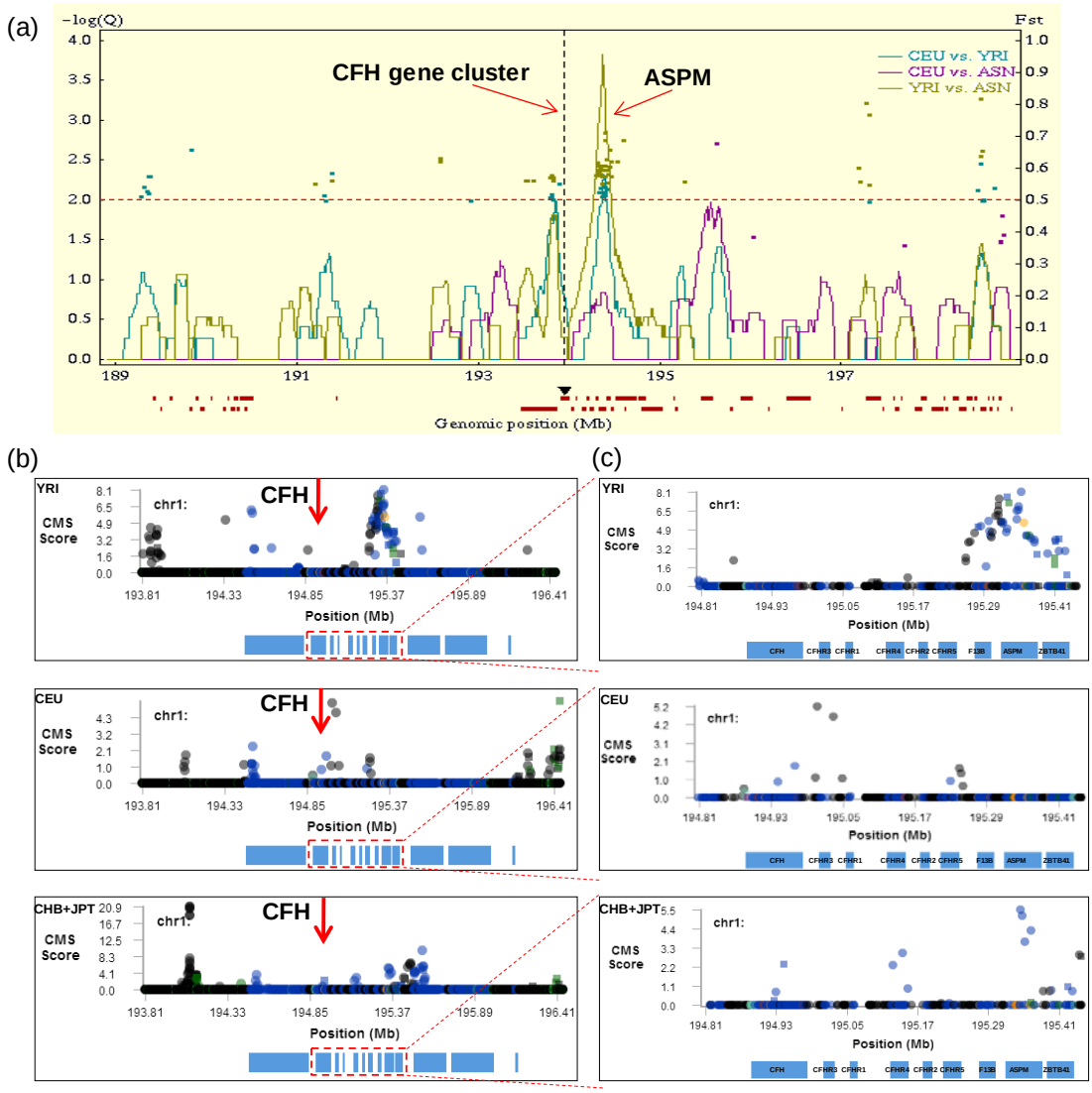

Figure S6. Positive selection on the *CFH* gene region. Two online tools for detecting positive selection in human genome were used: Haplotter **(a)** (http://haplotter.uchicago.edu/, using the HapMap data) and CMS viewer (**b-c**) (http://www.broadinstitute.org/mpg/cmsviewer/, using the 1000 genome data). Positive selection was observed in a region next to the *CFH* gene cluster in African (YRI) and Asian (CHB+JPT) populations, which contains the *ASPM* (abnormal spindle-like microcephaly associated) gene. The *CFH* region showed a signal of positive selection in European (CEU) population.

Acknowledgments

Data collection and sharing of the ADNI project was funded by the Alzheimer's Disease Neuroimaging Initiative (ADNI) (National Institutes of Health Grant U01 AG024904) and DOD ADNI (Department of Defense award number W81XWH-12-2-0012). ADNI is funded by the National Institute on Aging, the National Institute of Biomedical Imaging and Bioengineering, and through generous contributions from the following: Alzheimer's Association; Alzheimer's Drug Discovery Foundation; BioClinica, Inc.; Biogen Idec Inc.; Bristol-Myers Squibb Company; Eisai Inc.; Elan Pharmaceuticals, Inc.; Eli Lilly and Company; F. Hoffmann-La Roche Ltd and its affiliated company Genentech, Inc.; GE Healthcare; Innogenetics, N.V.; IXICO Ltd.; Janssen Alzheimer Immunotherapy Research & Development, LLC.; Johnson & Johnson Pharmaceutical Research & Development LLC.; Medpace, Inc.; Merck & Co., Inc.; Meso Scale Diagnostics, LLC.; NeuroRx Research; Novartis Pharmaceuticals Corporation; Pfizer Inc.; Piramal Imaging; Servier; Synarc Inc.; and Takeda Pharmaceutical Company. The Canadian Institutes of Health Research is providing funds to support ADNI clinical sites in Canada. Private sector contributions are facilitated by the Foundation for the National Institutes of Health (www.fnih.org). The grantee organization is the Northern California Institute for Research and Education, and the study is coordinated by the Alzheimer's Disease Cooperative Study at the University of California, San Diego. ADNI data are disseminated by the Laboratory for Neuro Imaging at the University of Southern California.

References

Bertram L, McQueen MB, Mullin K, Blacker D, Tanzi RE (2007). Systematic meta-analyses of Alzheimer disease genetic association studies: the AlzGene database. *Nat Genet* **39**: 17-23.

Bi R, Zhang W, Yu D, Li X, Wang HZ, Hu QX, *et al* (2015). Mitochondrial DNA haplogroup B5 confers genetic susceptibility to Alzheimer's disease in Han Chinese. *Neurobiol Aging* **36**: 1604 e1607-1604 e1616.

Bi R, Zhao L, Zhang C, Lu W, Feng JQ, Wang Y, *et al* (2014). No association of the LRRK2 genetic variants with Alzheimer's disease in Han Chinese individuals. *Neurobiol Aging* **35**: 444 e445-449.

Blalock EM, Geddes JW, Chen KC, Porter NM, Markesbery WR, Landfield PW (2004). Incipient Alzheimer's disease: microarray correlation analyses reveal major transcriptional and tumor suppressor responses. *Proc Natl Acad Sci U S A* **101**: 2173-2178.

Colantuoni C, Lipska BK, Ye T, Hyde TM, Tao R, Leek JT, *et al* (2011). Temporal dynamics and genetic control of transcription in the human prefrontal cortex. *Nature* **478**: 519-523.

Dale AM, Fischl B, Sereno MI (1999). Cortical surface-based analysis. I. Segmentation and surface reconstruction. *Neuroimage* **9**: 179-194.

Feng YM, Jia YF, Su LY, Wang D, Lv L, Xu L, *et al* (2013). Decreased mitochondrial DNA copy number in the hippocampus and peripheral blood during opiate addiction is mediated by autophagy and can be salvaged by melatonin. *Autophagy* **9**: 1395-1406.

Fischl B, Sereno MI, Dale AM (1999). Cortical surface-based analysis. II: Inflation, flattening, and a surface-based coordinate system. *Neuroimage* **9**: 195-207.

Fischl B, van der Kouwe A, Destrieux C, Halgren E, Segonne F, Salat DH, *et al* (2004). Automatically parcellating the human cerebral cortex. *Cereb Cortex* **14**: 11-22.

Harris JA, Devidze N, Verret L, Ho K, Halabisky B, Thwin MT, *et al* (2010). Transsynaptic progression of amyloid-beta-induced neuronal dysfunction within the entorhinal-hippocampal network. *Neuron* **68**: 428-441.

Higgins JP, Thompson SG (2002). Quantifying heterogeneity in a meta-analysis. *Stat Med* **21**: 1539-1558.

Khan UA, Liu L, Provenzano FA, Berman DE, Profaci CP, Sloan R, *et al* (2014). Molecular drivers and cortical spread of lateral entorhinal cortex dysfunction in preclinical Alzheimer's disease. *Nat Neurosci* **17**: 304-311.

Lambert JC, Ibrahim-Verbaas CA, Harold D, Naj AC, Sims R, Bellenguez C, *et al* (2013). Meta-analysis of 74,046 individuals identifies 11 new susceptibility loci for Alzheimer's disease. *Nat Genet* **45**: 1452-1458.

Purcell S, Neale B, Todd-Brown K, Thomas L, Ferreira MA, Bender D, *et al* (2007). PLINK: a tool set for whole-genome association and population-based linkage analyses. *Am J Hum Genet* **81**: 559-575.

Ramasamy A, Trabzuni D, Guelfi S, Varghese V, Smith C, Walker R, *et al* (2014). Genetic variability in the regulation of gene expression in ten regions of the human brain. *Nat Neurosci* **17**: 1418-1428.

Ritchie MD, Hahn LW, Roodi N, Bailey LR, Dupont WD, Parl FF, *et al* (2001). Multifactor-dimensionality reduction reveals high-order interactions among estrogen-metabolism genes in sporadic breast cancer. *Am J Hum Genet* **69**: 138-147.

The GTEx Consortium (2013). The Genotype-Tissue Expression (GTEx) project. *Nat Genet* **45**: 580-585.

Wang HZ, Bi R, Hu QX, Xiang Q, Zhang C, Zhang DF, *et al* (2014). Validating GWAS-Identified Risk Loci for Alzheimer's Disease in Han Chinese Populations. *Mol Neurobiol*.

Zhang DF, Wang D, Li YY, Yao YG (2014). Mapping genetic variants in the CFH gene for association with leprosy in Han Chinese. *Genes Immun* **15**: 506-510.